GEOLOGICA CARPATHICA, 2025, 76, 2, 117–136 https://doi.org/10.31577/GeolCarp.2025.06

Late Cenozoic stress states in the Datça and Bozburun Peninsulas, SE Aegean, Turkey

ALPER DEMIRCI[1,✉], SÜHA ÖZDEN[2], SEMIR ÖVER[3] and ERDEM GÜNDOĞDU[4]

[1]Çanakkale Onsekiz Mart University, Department of Geophysical Engineering, 17100, Çanakkale, Turkey
[2]Çanakkale Onsekiz Mart University, Department of Geological Engineering, 17100, Çanakkale, Turkey
[3]Iskenderun Technical University, Department of Civil Engineering, 31200, Iskenderun, Turkey
[4]Çanakkale Onsekiz Mart University, Vocational College, 17400, Çan, Çanakkale, Turkey

(Manuscript received January 27, 2025; accepted in revised form June 13, 2025; Associate Editor: Giovanni Barreca)

Abstract: The Datça and Bozburun are E–W-oriented peninsulas located near the Pliny–Strabo Trench Zone and considered to be eastern continuations of the seismically-active Hellenic Subduction Zone. Although no catastrophic earthquakes were recorded on the peninsulas in the previous century, two large earthquakes of a magnitude of 6.6 (Mw) occurred in the Gulf of Gökova in the north, in 2017, and a magnitude of 7.1 (Mw) in the Gulf of Fethiye in the south was recorded in 1957. Therefore, the necessity to pay close attention and issue warnings regarding potential earthquakes in and around the peninsulas has been increasing. Inversion of fault slip vectors affecting both the Plio–Quaternary and Paleozoic units in the Datça and Bozburun Peninsulas yields N–S, NE–SW, and NW–SE extensional stress states. The NW–SE trending Datça Basin formed during the Plio–Quaternary under the NE–SW extensional regime. The inversion of the focal mechanisms for shallow earthquakes in the Datça and Bozburun Peninsulas provides N–S and NW–SE extensional stress states. Extensional stress tensors obtained from both the fault planes measured, as well as the focal mechanisms of the shallow earthquakes, are related to the roll-back process of the African slab along the Hellenic Subduction Zone.

Keywords: Datça and Bozburun Peninsulas, late Cenozoic stress states, extensional, Hellenic Subduction Zone

Introduction

Interaction forces between the Arabian, African, and Eurasian plates, which are all in relative motion with one another, are to blame for the development of the extensional tectonic regime that is active in the Western Anatolia–Aegean region. These relative movements result in distinct forces at the plate boundaries, causing subduction in the south, extension in the west, and collision in the east of Anatolia (Fig. 1). Anatolia, which is located at the intersection of the plates, moves in a west-southwest direction along the dextral North Anatolian Fault Zone (NAFZ) in the north and the sinistral East Anatolian Fault Zone (EAFZ) in the east (McKenzie 1972; Dewey & Şengör 1979; Jackson & McKenzie 1984, 1988; Taymaz et al. 1991; McClusky et al. 2000). Although the extensional tectonics in the Western Anatolia–Aegean region are the result of a combination of plate boundary forces, many studies have demonstrated (Mercier et al. 1979; Royden 1993; Faccenna et al. 2004) that the force occurring in the subduction zone between Africa and Eurasia is more effective than others (Le Pichon & Angelier 1979; McClusky et al. 2000; Reilinger et al. 2010). As a result, it is assumed that slab retreat has dominant control on crustal extension, meaning that it reduces the horizontal stress on the overriding plate, as observed in the Andean Cordillera (Mercier 1981), as well as along the Eolian arcs (Malinverno & Ryan 1986), the Hellenic Arc (Le Pichon & Angelier 1979; Mercier et al. 1989), and the Cyprus Arc (Robertson 1990; Över et al. 2002).

Western Anatolia–Aegean is a region that is generally dominated by extensional regimes with different directions (Fig. 2). Although the main opening direction is N–S, both NW–SE and NE–SW directions have also been identified in a wider area (Alçiçek et al. 2006; Jolivet & Brun 2010; Brüstle et al. 2014; Över et al. 2016; Bocchini et al. 2018; Ocakoğlu et al. 2018; Kürçer & Gürsoy 2023). The ongoing extensional period began during the Miocene, creating dozens of basins with different directions and sizes: NW–SE, NE–SW, E–W, and N–S. The Edremit, Çandarlı, Kuşadası, Güllük, Gökova, and Hisarönü gulfs are associated with important east–west faults in the Western Anatolia–Aegean region. In the majority of geological, geophysical, and geodetic studies (Mercier et al. 1989; Taymaz et al. 1991; McClusky et al. 2000; Facenna et al. 2004; Reilinger et al. 2006, 2010; Biryol et al. 2011; Över et al. 2021), it has been emphasized that the effective extensional stress in Western Anatolia–Aegean is N–S. However, it is clear that the existence of faults with different directions, which indicates the complexity of the region, cannot be explained only by N–S extensional tectonics. The NE–SW and NW–SE extensional tectonic regimes within the complex tectonics of Aegean–Western Anatolia, in addition to the main N–S extensional regime, should be assessed in the context of the region's geodynamics.

✉ corresponding author: Alper Demirci
alperdemirci@comu.edu.tr

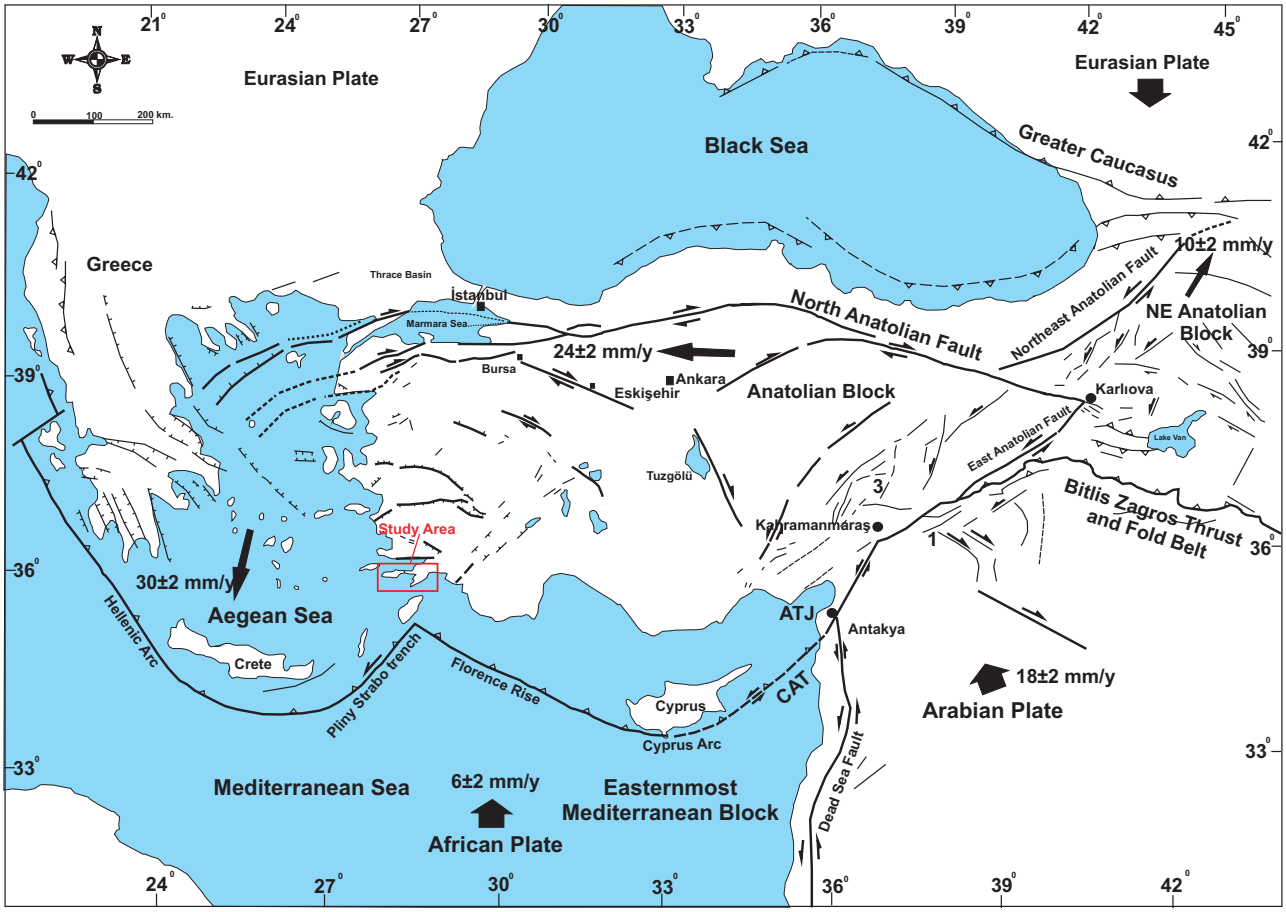

Fig. 1. Study area within the simplified tectonic framework of the eastern Mediterranean region (modified from Barka 1992; Barka & Reilinger 1997; Över et al. 2004, 2021). CAT: Cyprus–Antakya Transform Fault. ATJ: Antakya Triple Junction. Black arrows show the GPS velocity vectors from McClusky et al. (2000).

Ersoy (1990) and Dirik (2007) characterized the Datça Peninsula as a horst that is accompanied by a north dipping E–W trending, which is normal for the Datça Fault in the north, thereby defining the southern border of the Gökova Gulf. In the south, another E–W oriented normal fault dips to the south and forms the northern border of the Hisarönü (Gulf) Basin (Fig. 3). The Datça Graben, which has been tectonically active since the Pliocene (Özsayın et al. 2021) and located approximately in the center of the Datça Peninsula, is generally oriented in a NW–SE direction and thus required an NE–SW extension to form. The Kızlan Fault in the east and the Karaköy Fault in the south, both trending NW–SE, define the boundaries of the graben in question and offer an illustration of the area's tectonic complexity (Fig. 3).

The current study uses fault kinematic analysis and inversion of focal mechanisms of earthquakes that had occurred in the Datça–Bozburun Peninsulas in order to define stress states from the Pliocene to the present, as well as to determine their likely significance in relation to regional tectonic events. We believe that this study will contribute to a better understanding of the tectonic complexity of the region.

Geodynamic setting

The geodynamic environment of the eastern Mediterranean region represents the convergence of the Eurasian, African, and Arabian plates, all of which intersect in Turkey. The northward convergence of the African Plate leads to oceanic subduction along the Hellenic Arc (McKenzie 1972; Papazachos 1973; McClusky et al. 2000; Reilinger et al. 2010). The rate of motion of Western Anatolia–Aegean relative to Eurasia increases southward from 25 mm/year in the Aegean area to 35–40 mm/year at the Hellenic Arc, while Africa's northward migration is 10 mm/year (Le Pichon et al. 1995; McClusky et al. 2000; Reilinger et al. 2006, 2010). With a faster rate than the African Plate's relative northward migration, the leading edge of the African Plate subducts along the Hellenic Arc. As a result of the Mediterranean slab roll-back, the Hellenic Trench has been migrating southward relative to Eurasia and subducting beneath the Aegean Sea. Slab retreat in the Aegean domain and western Anatolia was attributed to the Mediterranean slab-pull force, which results in a reduction of horizontal stresses in the overriding plate (e.g., Le Pichon & Angelier

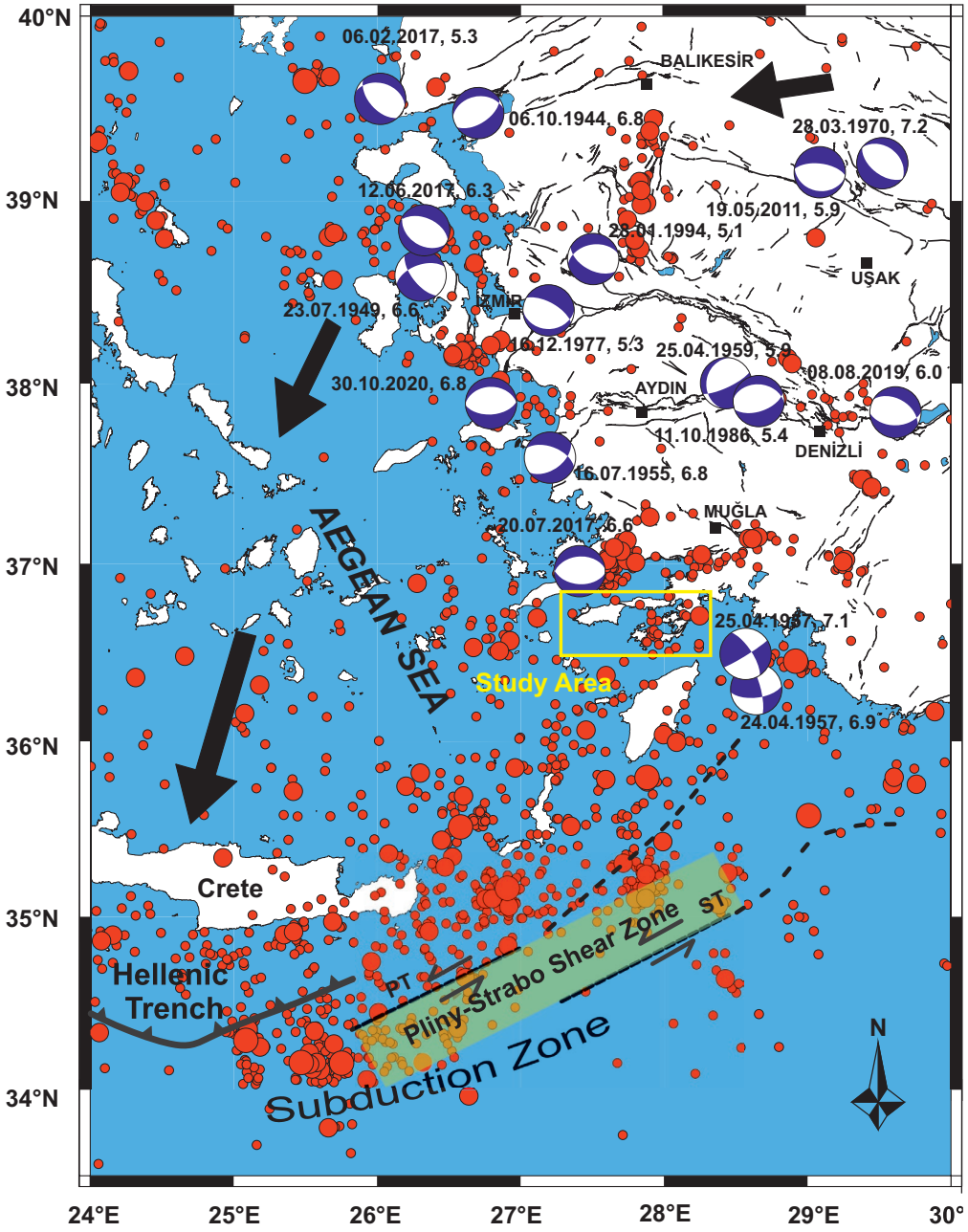

Fig. 2. Seismotectonic map of western Anatolia. Focal mechanism solutions of the regional earthquakes shown on the map (modified from Över et al. 2021). The blue balloons represent the focal mechanism solutions of some regional earthquakes shown on the map. Red circles give the seismicity of the region. Black arrows show the GPS Velocity vectors from McClusky et al. (2000).

1979; Le Pichon 1982; Mercier et al. 1989). According to the geodetically-determined velocity field of today, the Rhodes block, which is located in the southeast of the Aegean region, is moving toward the southeast at rates of up to 10 mm/yr in relation to the western, central, and southern Aegean regions, as well as others (Reilinger et al. 2010). Crustal extension in this region is usually consistent with independent GPS data (e.g., Le Pichon et al. 1995; McClusky et al. 2000; Reilinger et al. 2006 and 2010), earthquake focal mechanisms, and geological structures (e.g., McKenzie 1972; Jackson & McKenzie 1984; Taymaz et al. 1991; Facenna et al. 2004; Jolivet & Brun 2010; Papazachos et al. 2010; Brüstle et al. 2014; Bocchini et al. 2018). The Mediterranean slab-pull effect, which lowers the horizontal stresses in the overriding plate and causes broad extensional tectonics in the Aegean region and western Anatolia, has been associated with this slab retreat (e.g., Le Pichon & Angelier 1979; Le Pichon 1982; Sorel et al. 1988; Mercier et al. 1989).

According to recent plate kinematics and the significant curvature of the plate boundary, there is increasing obliquity in

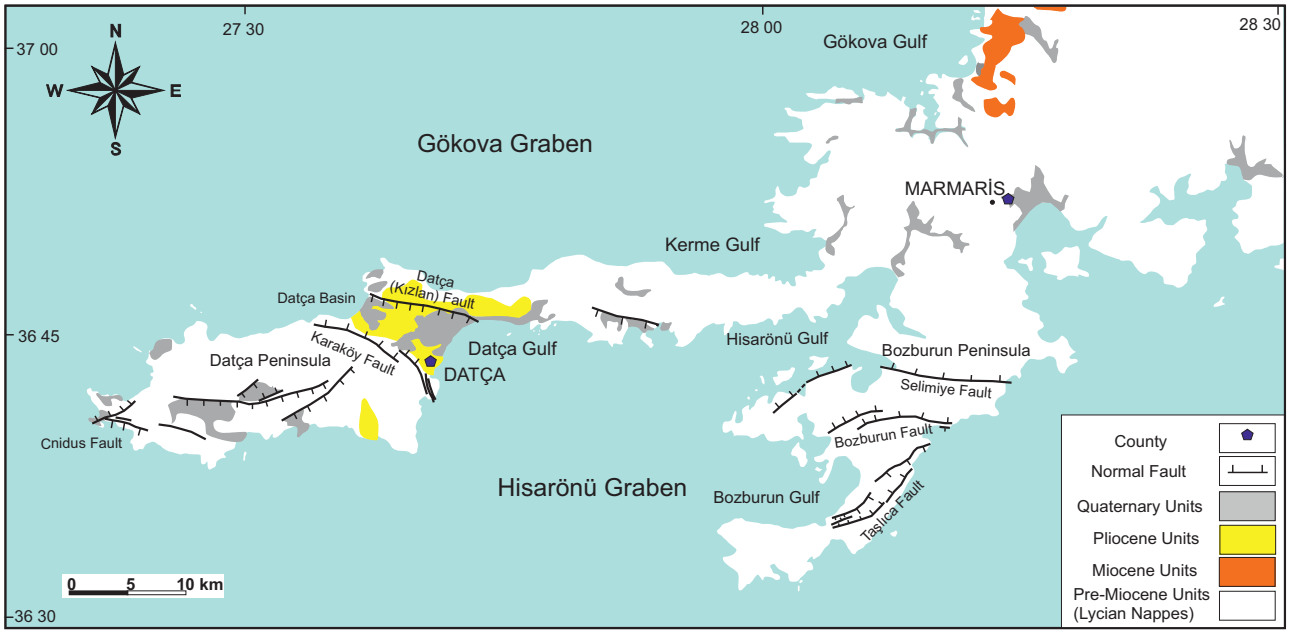

Fig. 3. Geological and active fault map of the Datça and Bozburun Peninsulas (modified from Şenel 1997; Emre et al. 2013; Özsayın et al. 2021).

the plate convergence from west to east in the Hellenic Subduction Zone. Left lateral motion occurs near the limits of the forearc due to the growing convergence slope that runs from the south to the east of Crete, particularly in the Rhodes region (Bohnhoff et al. 2006). The Ptolemy, Pliny, and Strabo trenches, which are in echelon bathymetric troughs that delineate these forearc limits, are thought to have formed as a result of the slab's continuous rollback and the oblique slide between Rhodes and Crete (ten Veen & Kleinspehn 2002; Meier et al. 2007). The direction of relative motion and the consistency of slip vectors from thrust earthquakes (Shaw & Jackson 2010) suggest that the Pliny–Strabo "trenches" support the oblique Africa–Aegean convergence. Certain studies that employ seismic tomography contend that the eastern extension of subduction necessitates the tearing of the subduction plate (Wortel & Spakman 2000; Biryol et al. 2011). The Pliny–Strabo plate boundary zone was defined simply as a strike-slip zone (Reilinger et al. 1997, 2006; Seyitoğlu et al. 2024) or was proposed to be a component of a subduction-transform-edge-propagator (STEP) fault surface expression linked to STEP activity at the border of the retreating African Plate. This vast deformation zone is commonly referred to as the "STEP fault" (Baes et al. 2011; Özbakır et al. 2013). Marine geophysical research has provided abundant evidence of left-lateral strike-slip motion on both the Pliny and Strabo trenches (Leite & Mascle 1982; Mascle et al. 1982). Numerous investigations (e.g., Govers & Wortel 2005; Dilek & Altunkaynak 2009; van Hinsbergen et al. 2010; Biryol et al. 2011; Özbakır et al. 2013; Govers & Fichtner 2016) showed the presence of a NE–SW trending STEP fault in the eastern part of the Hellenic Subduction Zone. However, many studies based on receiver function analysis, as well as seismicity, indicate the presence of a NW-dipping slab in the same region, particularly between Rhodes and Crete (Knapmeyer 1999; Papazachos et al. 2000; Brüstle et al. 2014; Sodoudi et al. 2015; Bocchini et al. 2018). This conflict is a good example of how complex the region where the Pliny–Strabo trenches are located has with a structure that still needs to be resolved. The stress tensors observed in this study do, however, reflect the geodynamic consequences of the Hellenic Subduction Zone, which should not be disregarded.

Seismicity

Historical records show that there is typically a lot of seismic activity along the Aegean coast, and that this activity is strong near the Datça and Bozburun Peninsulas (Ergin et al. 1967; Guidoboni et al. 1994; Ambraseys & White 1997; Yolsal et al. 2007). Intense micro-earthquake activity was measured off the coast of the Datça–Bozburun Peninsulas (Gürsoy et al. 2022). There are many tectonically-important, east–west gulfs on the Aegean coast that were shaken by earthquakes greater than 6.0 in the last century. On July 20, 2017, an earthquake of a magnitude of 6.8 (Mw) struck the Bodrum–Kos area north of the Gökova Gulf (Fig. 2). According to the cited sources, the northern region of the Gökova Gulf is more active compared to the Datça and Bozburun Peninsulas located to the south and the Hisarönü Gulf located further to the south. The majority of disastrous earthquakes, documented in A.D. 141, 144, 174, 344, 1493, 1851, and 1869 and 1999, 412, 227, and 24 B.C. (Ergin et al. 1967; Guidoboni et al. 1994; Ambraseys &

White 1997; Yolsal et al. 2007), took place in the northern section of the Gulf of Gökova. According to Luttrell (1999), the 1493 earthquake completely destroyed the city of Bodrum. Numerous medium-sized earthquakes, as well as earthquakes with a magnitude greater than 6.0 (in Mw) recorded during the instrumental period, indicate that the area is still active today. Examples include the earthquakes on December 13, 1941 (Mw: 6.3), April 25, 1959 (Mw: 6.2), and April 23, 1933 (Mw: 6.4) (Eyidoğan & Barka 1996; Uluğ et al. 2005; Yolsal & Taymaz 2010). On April 24, 1957, an earthquake with a magnitude of 7.1 (Mw) struck Fethiye Bay, which is situated south of the study area near the Pliny–Strabo trenches (Fig. 2). The last earthquake, which occurred on July 20, 2017 with a magnitude of 6.6, also occurred in the north of the Gulf of Gökova between Bodrum and Kos (Karasözen et al. 2018; Ocakoğlu et al. 2018; Tiryakioğlu et al. 2018). Kandilli Observatory and Earthquake Research Institute (KOERI) records show that over 3000 aftershocks with magnitudes ranging from 1.0 to 4.8 occurred throughout the Gulf of Gökova. The data does not follow a linear distribution and were scattered over a wide area, mostly in the west of the Gökova Basin and occasionally as far south as the Datça Peninsula (fig. 10 in Över et al. 2021). Although there is no data indicating that the Datça Peninsula and its near surroundings were the epicenter for any large destructive historical earthquake, records report that it was negatively affected by many destructive historical earthquakes (Çelikkol 1990, 1992; Ambraseys 1994; Ambraseys & Finkel 1995). Despite the absence of a destructive earthquake during the instrumental period, Figure 2 shows data indicating that the Datça Peninsula and its surroundings are quite active, although no large earthquake has affected this location during the instrumental period. This indicates a seismic gap in Datça–Bozburun and the surrounding area. In addition, it should not be overlooked that in the future the Datça–Bozburun region may be subject to a similar catastrophic disaster like the destructive earthquakes that have struck other regions of the Aegean coast.

Methodology

Focal mechanism solutions

In order to gain valuable insights into the regional deformation process, analyzing the full waveform is essential for the accurate determination of focal mechanisms. We used three-component broadband data from Turkey's regional network operated by the Kandilli Observatory and Earthquake Research Institute (KOERI). Our approach to determining earthquake mechanisms involves employing the iterative deconvolution method of Kikuchi & Kanamori (1991) via ISOLA software (Sokos & Zahradnik 2008) for 14 events with magnitudes between 3.9 and 6.6. We selected seismograms with good data quality. The minimum number of broadband stations used for the calculations is 6. After the instrumental correction of raw data for each station, we obtained the displacement seismograms by integration in the time domain. Determination of moment tensors involves minimizing the differences between synthetic and observed waveforms using the least-squares method. Synthetic seismograms were generated using Green's functions within the Fortran code of ISOLA, as well as by employing the discrete wavenumber method (Bouchon 1981). This method operates in the time-domain with the lowest feasible frequency, thus mitigating the impact of inaccuracies in the subsurface crustal model. The calculation of Green's functions using this methodology is suitable for both regional and local seismic events (Sokos & Zahradnik 2008).

The method provides moment tensor solutions through a spatiotemporal grid search that is performed in two stages in order to determine the optimum source location and time. First, we performed calculations at different depths with a depth range of 1 km and a time width of ±3 seconds, with 0.1 second increments around the origin time and keeping the epicenter coordinate fixed. In the second stage, with lateral plane grid spacings of 2×2 km for the obtained optimum depths, we accepted the solution with the lowest error rate (highest VR and DC ratio) as the solution for the relevant earthquake. The waveforms were subjected to band-pass filtering within the frequency range of 0.02–0.1 Hz. For this analysis, the crustal model utilized was derived from the velocity model proposed by Akyol et al. (2006) for Western Anatolia. Figure 4 presents the solution derived from the data for an event, which had a 4.2 magnitude and took place on January 25, 2017 at 01:19 (UCT), along with a comparison of observational and synthetic waveform fits (Fig. 4).

Fault kinematic analysis

Over the past 30 years, the fault slip inversion methodology has been employed in numerous active tectonic locations throughout the world in order to establish the state of stress and the evolution of late Cenozoic stress states (Över et al. 2010, see references therein).

Fault slips, which are sometimes referred to as striations that accumulate on fault lines, are inverted to determine the paleostress that impacted past geological formations (from the Pre Miocene to the Mio–Pliocene as well as Plio–Quaternary). For the population of fault planes recorded in the Datça Peninsula, an inversion approach developed by Carey (1979) was employed to compute the state of stress accountable for the late Cenozoic stress regime. Calculating the slip vectors (or striations) observed on fault planes yields the kinematics of the fault population. The deviator stress tensor can be calculated by inverting the measured slip vectors (Carey 1979; Angelier 1984) if the slip vector responsible for striations on each fault plane is in the direction and sense of the shear stress resolved (Bott 1959).

This method assumes that the shear stress determined for each fault plane is parallel to and moving in the same direction as the movement between solid blocks on the fault plane. Therefore, by reducing the angular deviation between the

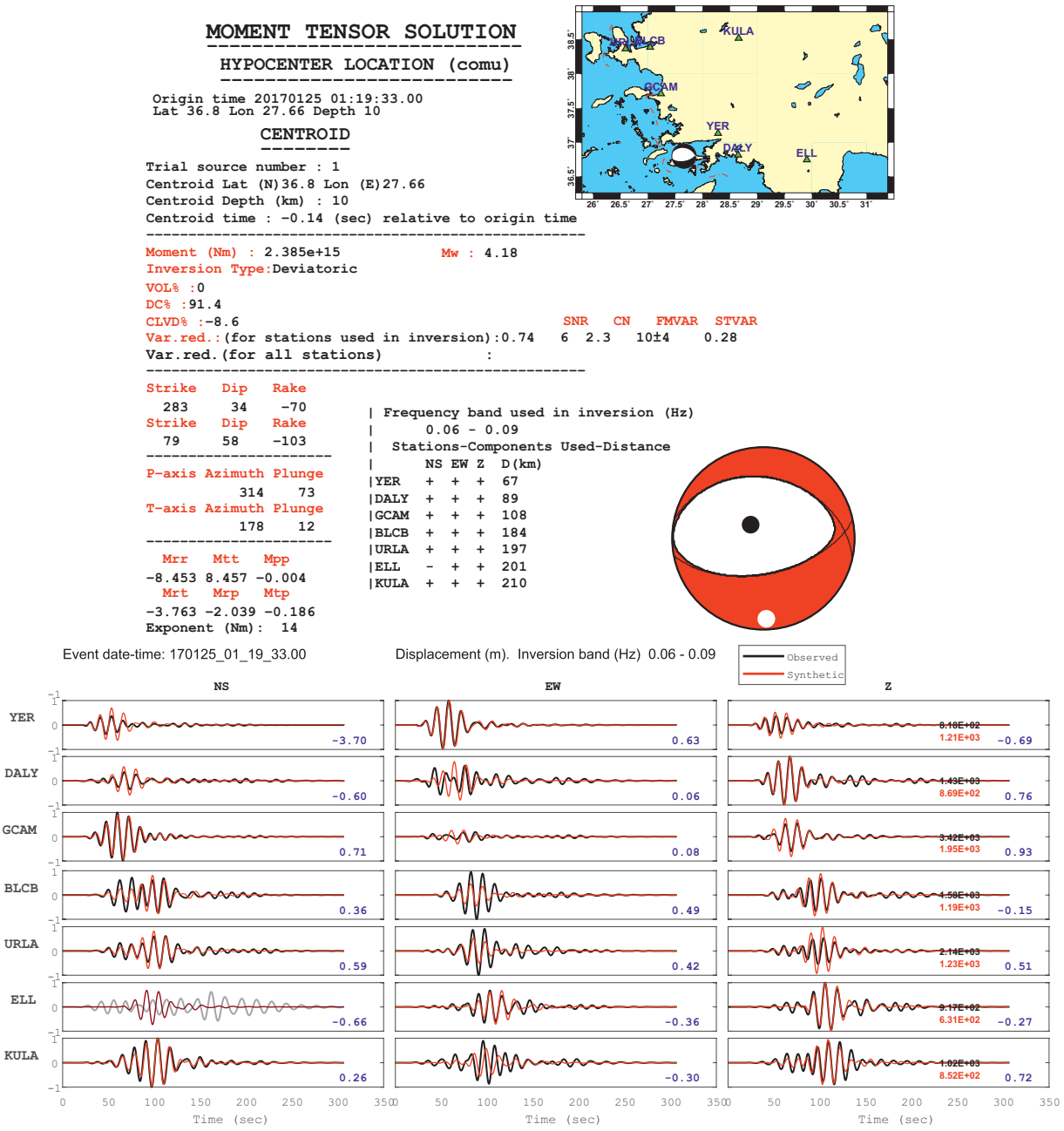

Fig. 4. MT solution result for Mw: 4.2 (25.01.2017; number 13 in Fig. 5 and Table 1) with synthetic waveform fits.

predicted slip vector (maximum shear, τ) and the measured slip vector (s), the best-fitting deviator stress tensor can be found (Carey & Brunier 1974; Carey 1979; Angelier 1984). Inversion outcomes include the stress ratio (R) and orientation (azimuth and plunge) of the primary stress axes for a mean deviation stress tensor. The stress magnitudes of the computed mean deviatoric stress tensor are described by the stress ratio, which is determined by the formula $[(R=(\sigma_2-\sigma_1)/(\sigma_3-\sigma_1)]$. In fact, the shape of a stress ellipsoid is determined by its stress ratio. The compressional, intermediate, and extensional deviatoric stress axes correspond to the principal stress axes σ_1, σ_2, and σ_3, respectively. The R ratio is a scalar number that defines the shape of the stress ellipsoid by describing the deviatoric stress magnitude, where $|\sigma_1+\sigma_2+\sigma_3|=0$. Bellier & Zoback (1995) explored the importance of the stress ratio in interpreting inversion data. As mentioned, the two end-member uniaxial stress states (R=0 when $\sigma_2=\sigma_1$ and R=1 when $\sigma_2=\sigma_3$) result in different changes in the stress ratio R.

When dipping faults of all orientations have an R=1 end-member, it means that the two horizontal stresses are equal (radial extension) and the predicted deformation is pure normal (down dip) slip in a normal faulting stress regime, where vertical stress $\sigma_v=\sigma_1$, maximum horizontal stress $\sigma_{Hmax}=\sigma_2$, and minimum horizontal stress $\sigma_{Hmin}=\sigma_3$. On the other hand,

the R=0 endmember suggests a stress state transitional from normal faulting to strike-slip, since it shows that the maximum horizontal and vertical stresses are equal ($\sigma_{Hmax}=\sigma_v$). Additionally, low R values (R<0.15) imply a close transition from normal faulting to strike-slip, whereas high R values (R>0.85) indicate a stress state with near uniform radial extension (Bellier & Zoback 1995). The results of stress inversions are normally deemed accurate if 80 % of the deviation angles (angle between the estimated slip vector and measured slip vector) are less than 20 degrees (Carey 1979).

Kinematic analysis of focal mechanism solutions

It is possible to determine the regional stress tensor responsible for current deformations by using the focal solution mechanisms of earthquakes that have occurred in a given area (Carey-Gailhardis & Mercier 1987). The earthquake focal solution structure is made up of two planes: the fault and the auxiliary perpendicular plane (also known as nodal). However, the true fault plane and the auxiliary plane can be distinguished from one another by the surface rupture, the spatial distribution of aftershocks, or computer-aided numerical analysis. Numerical methods were developed to identify which of the nodal planes is the fault plane (Angelier & Mechler 1977; Carey-Gailhardis & Mercier 1987). Actually, the genuine fault plane, which carries the slip vector and corresponds to the principal stress orientations, can be determined using Bott's (1959) model and is one of the two nodal planes identified in the earthquake focal analysis. The calculated stress ratio [$(R=(\sigma_2-\sigma_1)/(\sigma_3-\sigma_1)$] should be between 0 and 1, and the seismic shear vector must be compatible with the stress tensor. While the auxiliary plane does not meet this requirement, the seismic plane from the nodal plane does, but only if both planes do not contact one another along a primary stress vector (Carey 1979).

The major goal of using the fault kinematic method is to assess the Plio–Quaternary stress regime and its importance for the regional tectonic phase. Kinematic analysis of faults identified in the Datça Peninsula was carried out to acquire better knowledge of regional tectonics. For the past 40 years, the fault kinematic analysis approach to evaluate paleostress has been used in active tectonic studies all over the world (e.g., Angelier et al. 1981; Mercier et al. 1991; Bellier et al. 1997; Över et al. 2010), thereby contributing to the improvement of knowledge of regional tectonics acting in the relevant field.

Results

Present-day stress state

Carey-Gailhardis & Mercier's (1987) inversion approach was employed for the focal mechanisms of earthquakes in the Datça region and its environs in order to develop a regionally-relevant stress tensor responsible for current faulting. A total of 22 earthquakes were used, including 14 source mechanisms with inversion performed using ISOLA in this study (Sokos & Zahradnik 2008) and 8 source mechanisms solved by USGS and NOA. Table 1 lists, and Figure 5 illustrates, the resolved focal mechanisms for earthquakes with a magnitude of 3.9 to 6.6 in the 1987–2024 period.

In the research area and its environs, the inverse solution of seismic fault slips derived from shallow earthquake focus solutions demonstrated the presence of both the dominant N–S extension and NW–SE extension. Inversion of 12 resolved seismic fault-slip sets resulted in a normal fault stress regime (SFM 1) with an approximately N–S (N3°E)-trending (σ_3) axis (Fig. 6a, Table 2). The inversion of focal mechanisms for 5 earthquakes gave a NE–SW (N115°E) extensional stress state (SFM 2; Fig. 6b, Table 2). The focal mechanisms of 5 earthquakes (balloons no: 1, 18, 19, 20 and 22 in Fig. 4 and Table 1) that occurred at a depth of more than 60 km for which CMT solutions were obtained indicate reverse faulting. The inversion of these deep reverse seismic fault slips indicates a NE–SW (N219°E) compressional stress state (SFM3, Fig. 6c, Table 2).

Late Cenozoic stress state

This study includes the results of all measurements carried out on rocks ranging from the early Cenozoic to the Plio–Quaternary. The fault planes measured in the region are obviously typical normal faults, as the sample photographs in Figures 7–11 make evident. Fault measurements were made in 14 places – 11 locations in the Datça Peninsula and 3 in the Bozburun Peninsula to the south (Fig. 12, Table 3). Site 2 was in Quaternary units; sites 3 and 4 were in Pliocene units; all the remaining locations were in the Pre-Neogene units (Table 3). On the Datça and Bozburun Peninsulas, inversion of the fault-slip vectors indicates normal faulting that correlates to locally and/or regionally important stress regimes. Results of all measurements from Pliocene to Quaternary rocks, as well as Paleozoic rocks, are included in this study (Table 3). The majority of inversions provide approximate N–S extension (NNE–SSW to NNW–SSE). However, the results at sites 2 and 5 demonstrate NE–SW extension, while the results at locations 4, 8, 13, and 14 show NW–SE extension (Figs. 12, 13 and Tables 2, 3).

Discussion

N–S extension is predominant in the Datça and Bozburun Peninsulas as well as their environs, as evidenced by the inversion of slip vectors that were gathered from fault planes and the inversion of seismic fault slips derived from the focal solutions of shallow earthquakes. Kinematic fault analysis performed in 8 out of 14 measurement locations shows the efficacy of the approximate N–S extension regime. Fischer's statistical results for the individual σ_{Hmin} (σ_3) axis in all 8 regions show an azimuth of 1 degree (N1°E) and a dip value

of 11 degrees. The arithmetic R value is 0.675. Inversion of the 11 resolved seismic fault-slip sets results in a normal fault stress regime with approximate N–S (N3°E) trending σ_{Hmin} (σ_3) axis and the calculated stress ratio R value is 0.824 (Fig. 6, SFM1). As stated by Bellier & Zoback (1995), radial extension stress conditions necessitate a high R value (R≥0.85). The computed R value of 0.824 indicates a triaxial extensional stress state and obviously varies from radial

Table 1: The parameters of the Datça–Bozburun Peninsulas and around earthquakes are given. Used nodal planes marked by bold characters are selected with the inversion method of Carey-Gailhardis & Mercier (1987).

No	Date	Origin Time (UTC)	Lat (Degree)	Long (Degree)	Mw	Depth (km)	NP1 (Str/Dip/Rake)	NP2 (Str/Dip/Rake)	Ref
1	19.06.1987	18:45:41	36.79	28.19	5.3	79.5	316/54/137	75/57/45	USGS
2	05.10.1999	00:53:28	36.73	28.24	5.2	33	**275/52/−34**	28/64/−136	USGS
3	04.08.2004	03:01:07	36.83	27.81	5.6	10	75/40/−96	**262/50/−85**	USGS
4	04.08.2004	03:49:32	36.79	27.83	4.4	10	**71/49/−99**	265/42/−80	This study
5	04.08.2004	04:19:48	36.84	27.85	5.2	10	71/42/−111	**278/52/−72**	USGS
6	04.08.2004	14:18:50	36.83	27.83	5.3	10	75/41/−94	**260/49/−87**	USGS
7	11.01.2005	04:36:00	36.92	27.87	5.1	35	**255/60/−103**	100/33/−69	USGS
8	19.06.2007	19:38:48	36.73	27.35	4.0	23	8/34/−125	**228/63/−68**	This study
9	08.08.2010	00:24:10	36.63	28.01	4.3	30	208/29/−153	**94/78/−64**	This study
10	04.06.2012	14:19:52	36.95	28.21	4.2	10	**51/59/−83**	217/32/−102	This study
11	24.11.2012	21:04:16	36.60	27.92	5.0	8	**239/79/−100**	101/15/−50	This study
12	26.11.2012	17:35:41	36.65	27.99	5.0	11	226/27/−130	**89/70/−72**	This study
13	25.01.2017	01:19:33	36.75	27.66	4.2	10	**283/34/−70**	79/58/−103	This study
14	20.07.2017	22:31:11	36.96	27.41	6.6	6	**89/50/−95**	277/40/−84	This Study
15	21.07.2017	03:59:02	36.80	27.59	4.1	10	285/22/−86	**101/68/−91**	This study
16	08.08.2017	07:42.22	36.96	27.57	5.3	10	48/49/−126	**276/53/−56**	This study
17	22.01.2019	20:12:06	36.81	28.00	4.8	14	23/21/−121	**236/72/−78**	This study
18	28.06.2020	17:43:28	36.75	28.25	5.4	63	329/56/149	**78/64/38**	USGS
19	29.06.2020	04:06:23	36.73	28.22	4.6	65	296/50/141	**53/61/48**	This study
20	21.08.2023	15:46:02	36.83	28.31	4.6	70	**8/63/159**	108/71/28	NOA
21	06.07.2024	10:09:22	36.68	28.11	3.9	30	146/42/−25	**255/74/−129**	This study
22	09.07.2024	12:11:50	36.70	28.15	4.5	81	**43/46/65**	257/49/114	This study

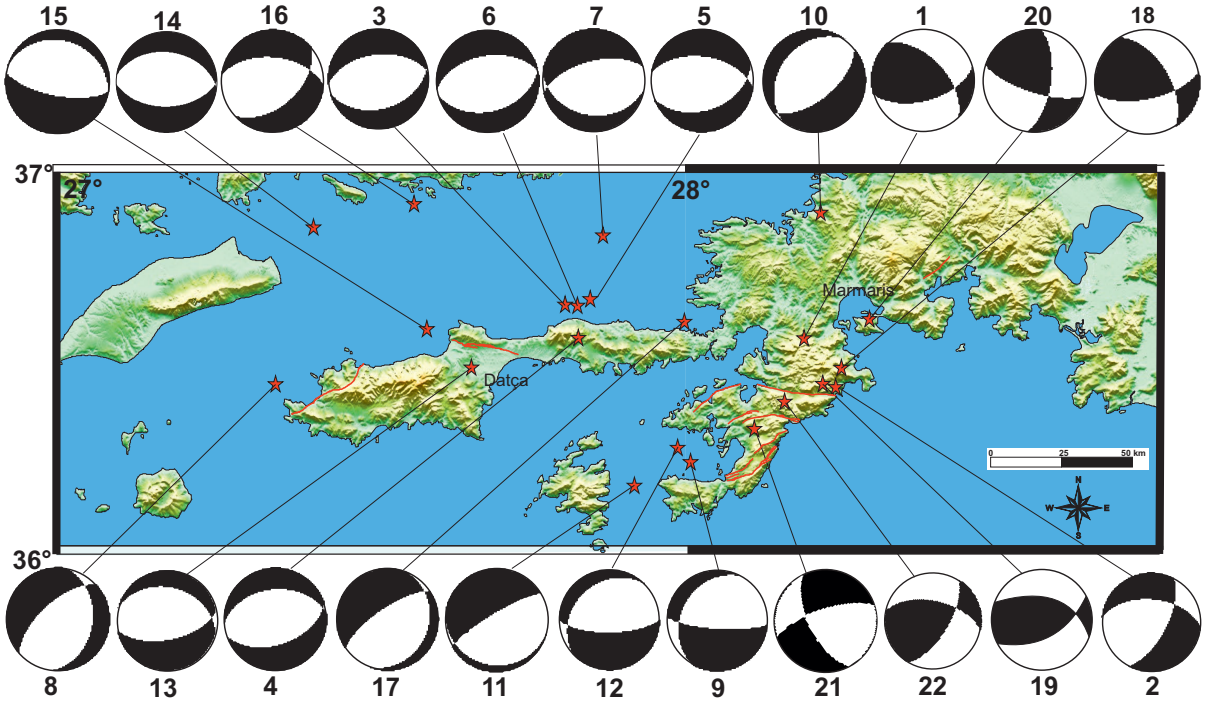

Fig. 5. Moment tensor solutions for 22 earthquakes (M>3.9) between 1987 and 2024. Red stars represent the epicenters of the events used in the inversion.

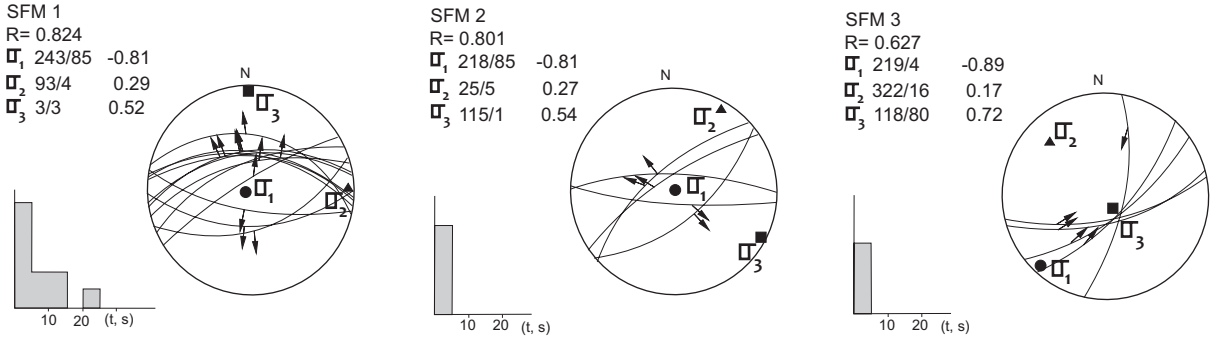

Fig. 6. Lower hemisphere stereoplots of the earthquake slip data with the present-day regional principal stress directions computed from the focal mechanisms of earthquakes shown in Fig. 3 and Table 1. The preferred seismic fault planes are chosen according to the method of Carey-Gailhardis & Mercier (1987). Black arrows on the seismic fault planes give the deviation angle between measured (s) and predicted (t) slip vectors on each fault plane. Two different directions normal faulting (SFM 1 and SFM 2) and reverse faulting (SFM 3) defines stress state in the study area as the results of the inversion. Histogram shows distribution of deviation angles (angle between the observed slip (s) and the predicted slip (t)).

conditions. Almost every study conducted in the Western Anatolia and Aegean region has revealed consistent results (e.g., Mercier et al. 1989; McClusky et al. 2000, 2003; Alçiçek et al. 2006; ten Veen et al. 2009; Sözbilir et al. 2011; Özden et al. 2018; Taymaz et al. 2022). However, the N–S extensional stress tensor alone is insufficient to adequately characterize and/or comprehend the complex tectonics of the region. The inversion of faults recorded in Pre-Neogene deposits resulted in a NW–SE extensional stress state (location number 3), whereas faults measured in Plio–Quaternary deposits resulted in NE–SW extensional stress. The inversion on faults measured in Pre-Neogene units at location 3 gives a NW–SE extensional stress state compatible with (N342°E) σ_{Hmin} (σ_3) axis. The R value is 0.90, indicating a radial extension stress state (site 3, in Fig. 12). Inversions at sites 1, 3, and 5 with high R values (Fig. 12) also show radial extension. Since this kind of deformation impacts the back-arc basins of subduction zones, the discovery of radial extension in the study area is not surprising (Philip 1987). During the Pleistocene period, radial extension related to subduction along the Tyrrhenian arc in the Mediterranean region was also noted in southern Calabria (Bousquet 1973). Inversion of five resolved seismic fault-slip sets gave NW–SE (N115°E) extension with R value of 0.80, suggesting a triaxial stress state. Both the Aegean and Western Anatolia regions have a large distribution of these various directions of extension.

The fundamental component of the complex structure in the study area is that explaining the deformation structures, which arise as a result of this extension, is not always simple and occasionally, not even possible. Alçicek et al. (2006) noted NW–SE and NE–SW extensions using biostratigraphy analysis, as well as tectono-sedimentary data from the Çameli Basin in SW Anatolia. They suggested that the Çameli Basin may have developed through NW–SE extension from the late Miocene to the Pliocene epoch. According to Över et al. (2010), the NW–SE and NE–SW extensions observed in SW Anatolia during a kinematic fault study are linked to subduction activities along the Hellenic and Cyprus arcs. The NW–SE extension is caused by the subduction process along the Cyprus arc, but a stronger NE–SW to N–S extension was formed by the combined forces of the subduction process along the Hellenic Arc and the southwestward extrusion of Anatolia. Thus, the NW–SE Datça Basin formed under the NE–SW extension in relation to the subduction process along the Hellenic Arc, as evidenced by the analysis of faults measured in Quaternary units in the north of the basin (sites 2

Table 2: Results of stress tensor inversions for slip data representing normal faulting stress state. SS 1 is an average stress state obtained from using Fisher statistics on individual σ_3 axis. Rm value is the calculated mean of all sites. SFM 1–3 is the stress state obtained from focal mechanism inversion. N column give the number of slips measured.

Sites	σ_1 (Az/dip)	σ_2 (Az/dip)	σ_3 (Az/dip)	R	N
1	76/79	273/11	182/3	0.926	7
2	213/65	319/7	53/24	0.645	5
3	72/78	252/13	342/11	0.909	11
4	79/79	259/11	169/0	0.885	5
5	135/86	301/4	31/1	0.933	5
6	51/72	279/12	187/13	0.628	8
7	163/73	73/9	343/14	0.435	4
8	4/67	250/12	155/24	0.467	10
9	286/64	79/24	174/10	0.877	9
10	200/76	109/19	19/17	0.621	12
11	281/72	95/18	186/2	0.819	6
12	134/71	263/12	356/14	0.369	4
13	154/71	64/10	334/8	0.511	4
14	359/67	239/12	145/19	0.420	5
SS 1	**σ_2=93°/12°**	**and**	**σ_3=175°/11°**	**R=0.80**	**39**
SS2	**σ_2=123°/12°**	**and**	**σ_3=35°/11°**	**R=0.733**	**22**
SS2	**σ_2=68°/12°**	**and**	**σ_3=156°/11°**	**R=0.55**	**34**
SFM 1	**σ_2=93°/4°**	**and**	**σ_3=3°/3°**	**R=0.824**	**12**
SFM 2	**σ_2=25°/5°**	**and**	**σ_3=115°/1°**	**R=0.801**	**5**
SFM 3	**σ_1=219°/4°**	**and**	**σ_2=322°/16°**	**R=0.627**	**5**

Fig. 7. Photographs show metric normal faults of the Pre-Neogene units (Cnidus Fault) in the Datça Peninsula measured at site 1 (Figs. 12, 13; Tables 1–3).

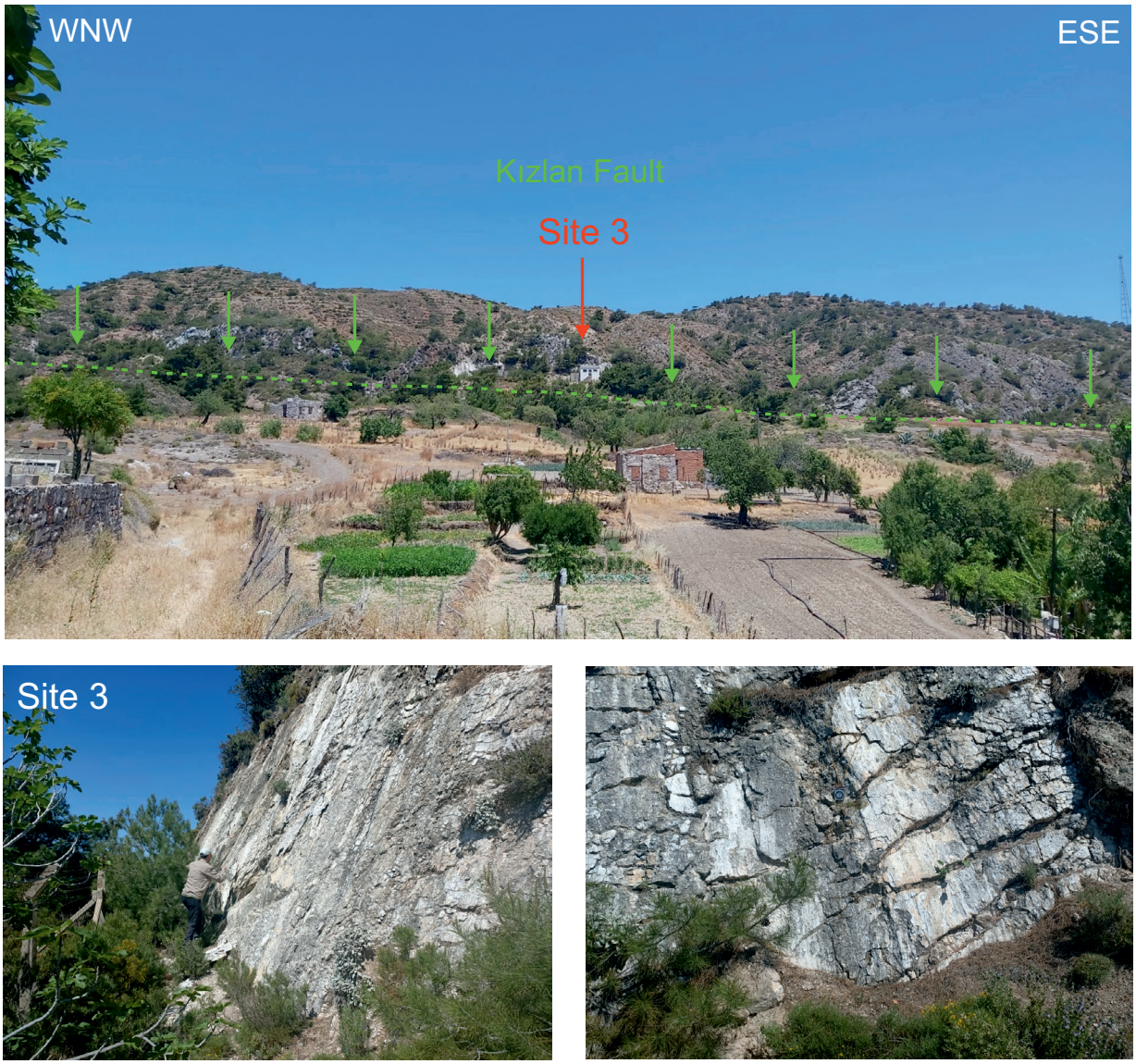

Fig. 8. Photographs show metric normal faults of the Pliocene units (Kızlan Fault) in the Datça Peninsula measured at site 3 (Figs. 12, 13; Tables 1 and 2).

and 5, in Fig. 13) and faults cutting Paleozoic units at the southwestern end of the basin (site 1, in Fig. 13).

Över et al. (2021) obtained N–S extension from available focal mechanisms of 58 events with a magnitude ranging from 4.0 to 6.6 between 1933 and 2017 as part of a Gulf of Gökova study related to the Bodrum–Kos earthquake (Mw:6.6) on July 20, 2017. In the same analysis, the focal mechanisms of 21 aftershocks that occurred at the NW end of the Gulf were inverted, resulting in a NW–SE (N330°E) trending (σ_3) axis (fig. 11b in Över et al. 2021). They concluded that the NW–SE extension was evaluated as a local stress state that most likely played a role in the development of the western region of the asymmetric Gökova Basin. The western part of the Gökova Basin is substantially quicker than the eastern part (Tur et al. 2015). Using inversion of the 67 nodal plane sets in the Gökova area, Shah (2015) identified a normal faulting stress regime (σ_1 is vertical) with a NW–SE (N313°E) σ_3 axis. He also proposed that the Gökova area can be identified by a counterclockwise rotation of stress directions from the N–S to the NW–SE. According to the seismic profile recorded from the east coast of the island of Kos in the northwest of the Gulf of Gökova, there are NE–SW oriented listric and synthetic faults (profile no. 3 in Ocakoğlu et al. 2018) that indicate NW–SE extension. Furthermore, active normal faults in the Symi Iceland (Soukis & Goulioti 2018), as well as in Karpathos and Rhodes (Mascle et al. 1986), demonstrate NW–SE extension, suggesting the relevance of NW–SE extension at the regional scale.

Seyitoğlu et al. (2024) proposed that the Pliny–Strabo fault zone influenced strike-slip faults measured on the Bozburun

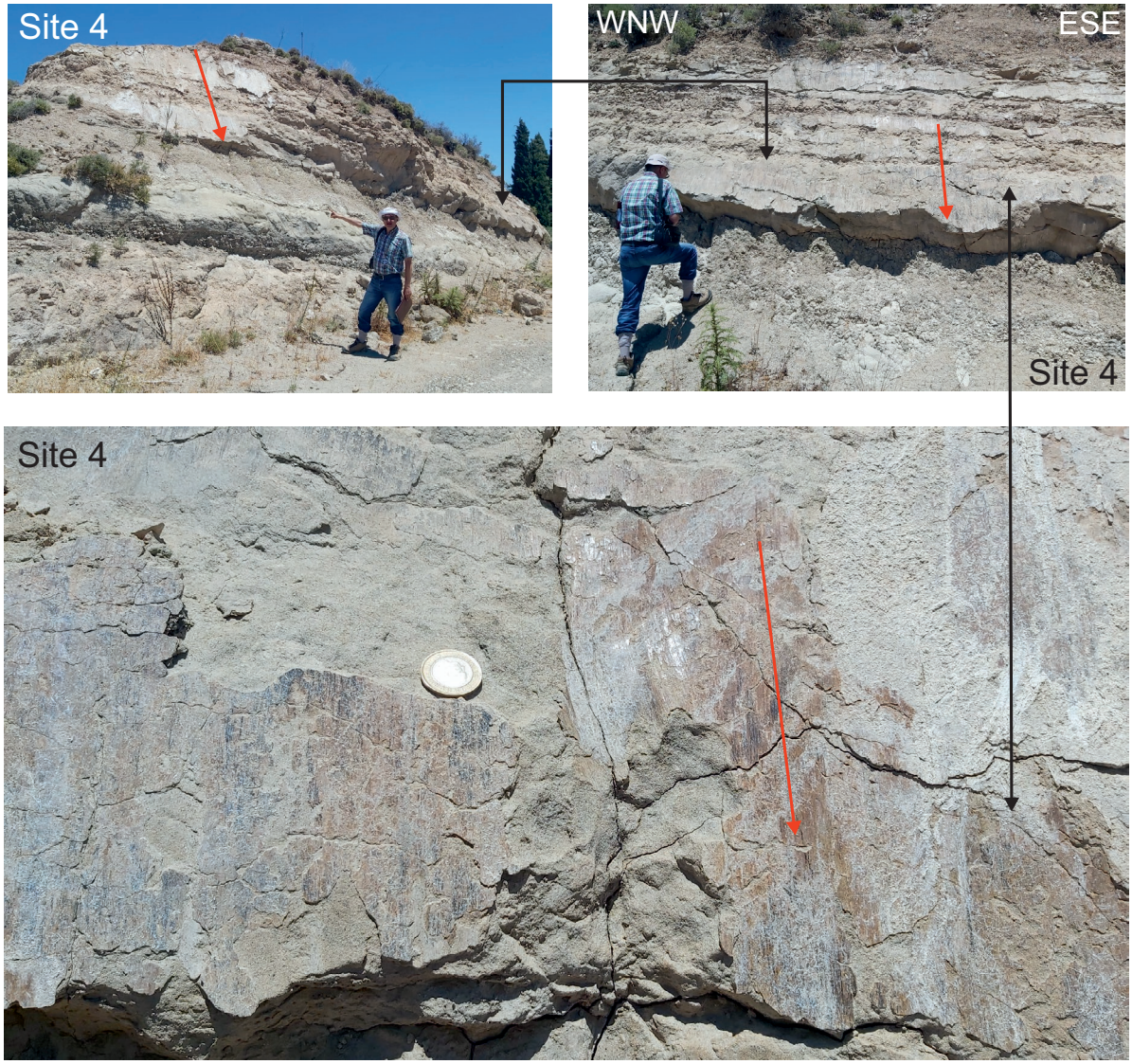

Fig. 9. Photographs show metric normal faults of the Pliocene units (Kızlan Fault) in the Datça Peninsula measured at site 4 (Figs. 12, 13; Tables 1 and 2).

Peninsula. The Fethiye–Burdur Fault, which is the Pliny–Strabo Fault's onshore continuation, was regarded as the most significant strike-slip system representative in Southwest Anatolia (Reilinger & Barka 1997). However, both tectono-sedimentary investigations (ten Veen et al. 2004, 2009; Alçiçek et al. 2006) and microtectonic studies based on kinematic fault analysis (Över et al. 2010, 2013a, b, 2016) demonstrate that the Fethiye–Burdur Fault Zone has no strike-slip character. Despite this, they identified it as a normal fault. McClusky et al. (2000) observed three velocity vectors in SW Turkey relative to Anatolia (fixed), specifically in the southern part of the FBFZ: two vectors show S-trending migration, while a third vector in the easternmost section (near Antalya) indicated SE migration from SW Anatolia. These velocity vectors support extensional tectonics along the FBFZ, and according to Över et al. (2010), the subduction process occurring along the Cyprus Arc is responsible for the SE movement. In future studies on the source of NW–SE extensional stress states obtained both at the NW end of Gökova Bay (Över et al. 2021) and in the Datça–Bozburun Peninsula (current study), the effect of the subduction process in and around the Pliny–Strabo region should not be ignored.

A shallow earthquake with magnitudes of 7.4 occurred on July 9, 1956, southwest of Amorgos Island in the southern Aegean (Fig. 14). The focal mechanism of this major event, which occurred in the Hellenic Subduction Zone, displays a normal character with a SE-oriented T axis (Comninakis & Papazachos 1986; Macropolos et al. 1989; Okal et al. 2009; Brüstle et al. 2014). Based on the focal mechanisms of the earthquakes (Mw≥5.0) throughout the eastern portion of the Hellenic Arc, Bocchini et al. (2018) obtained a NW–SE extensional regime from the focal mechanisms of earthquakes

Fig. 10. Photographs show metric normal faults in the Datça Peninsula measured at site 9–10 (Figs. 12, 13; Tables 1 and 2).

(Mw≥5.0) along the eastern part of the Hellenic Arc. As a result, they proposed the idea of detachment of the Rhodes block from the Central Aegean region. The analyses of well-located hypocenters from EGELADOS and CYCNET temporary network catalogues were used to examine the geometry of the slab in the southeast Aegean, where a number of studies reported a dramatic increase in the slab dipping angle (Papazachos & Nolet 1997; Meier et al. 2007; Brüstle 2012; Sodoudi et al. 2015). From the seismicity cross-sections from temporary network catalogues (EGELADOS and CYCNET), Bocchini et al. (2018) revealed that the area around Crete has a shallower and less-seismically active N-NNE dipping slab, while the area around Karpathos–Rhodes has a steeper and more seismically active NW dipping slab. The GPS velocity field in relation to the central and southern Aegean (fixed), which confirms the SE motion of the southeast region of the Aegean towards the Hellenic Subduction Zone, i.e., Pliny–Strabo Trenches Zone (fig. 2 in Reilinger et al. 2010 and fig. 8 in McClusky et al. 2000). The GPS vector observed in the western section of the Datça–Bozburun Peninsulas indicates

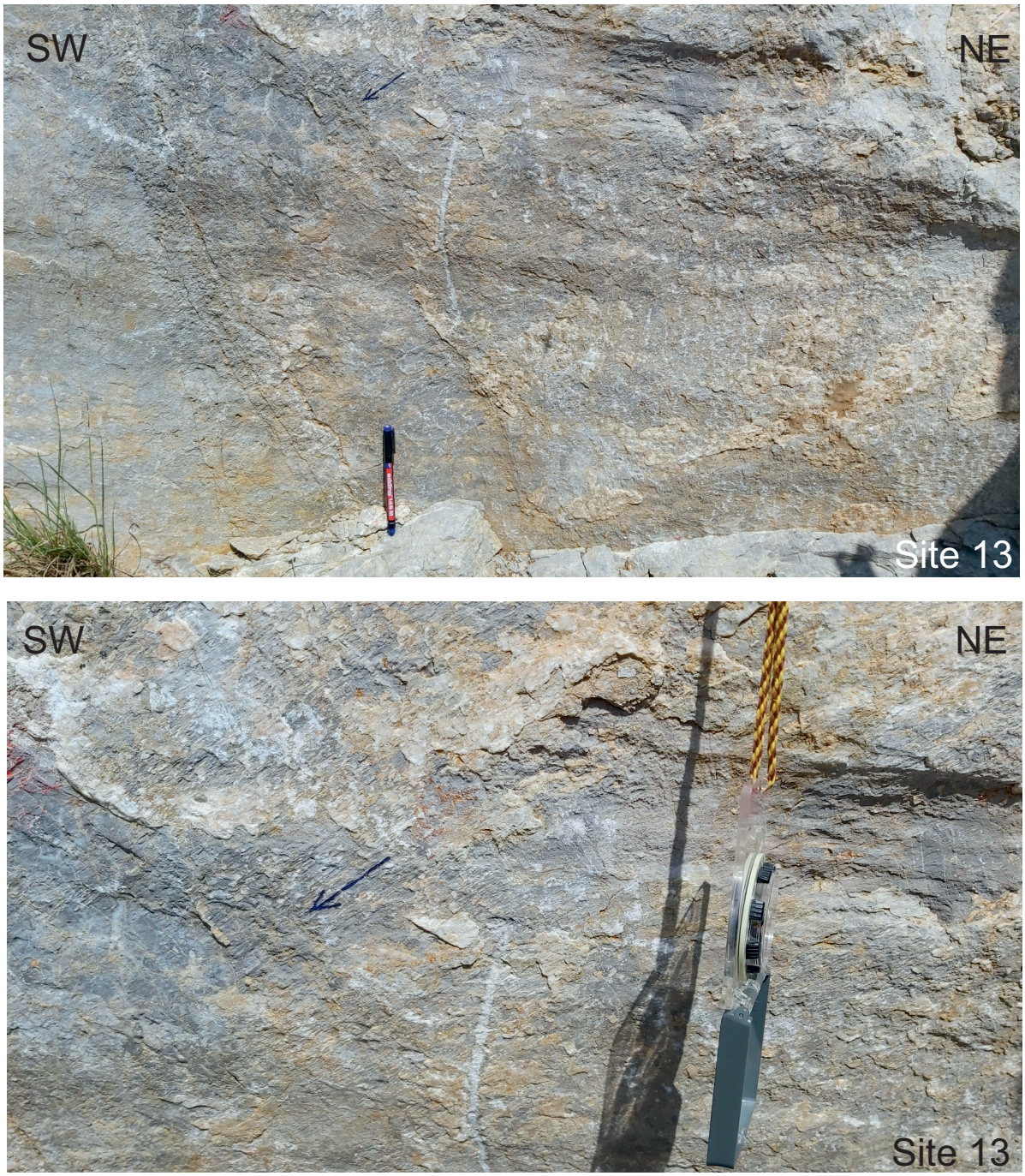

Fig. 11. Photographs show oblique normal fault in the Bozburun Peninsula measured at site 13 (Figs. 12, 13; Tables 1 and 2).

SE trending movement of the peninsula, showing the influence of the pull-force in relation to the eastern part of the Hellenic Subduction Zone (Fig. 14). This lends support to the hypothesis that NW–SE extension detected in the SE Aegean can be attributed to subduction events along the eastern segment of the Hellenic Subduction Zone, at least between Rhodos and Crete. In conclusion, the N–S to NE–SW extension resulted from the roll-back process that occurred along the Hellenic Trench, while the NW–SE extension is caused from the roll-back process that occurred along the eastern part of the Hellenic Subduction Zone.

One of the most important results of the study is that 4 deep earthquakes (earthquakes no. 1, 18, 19, 20, and 22; Fig. 5 and Table 1) occurred in the eastern part of the Bozburun Peninsula at a depth of >60 km. The calculation yields a NE–SW compressional stress state compatible with N221°E σ_{Hmax} (σ_1) axis (SFM3 in Fig. 5). One of the greatest earthquakes in the southern Aegean, with a magnitude of Ms: 7.4, and another

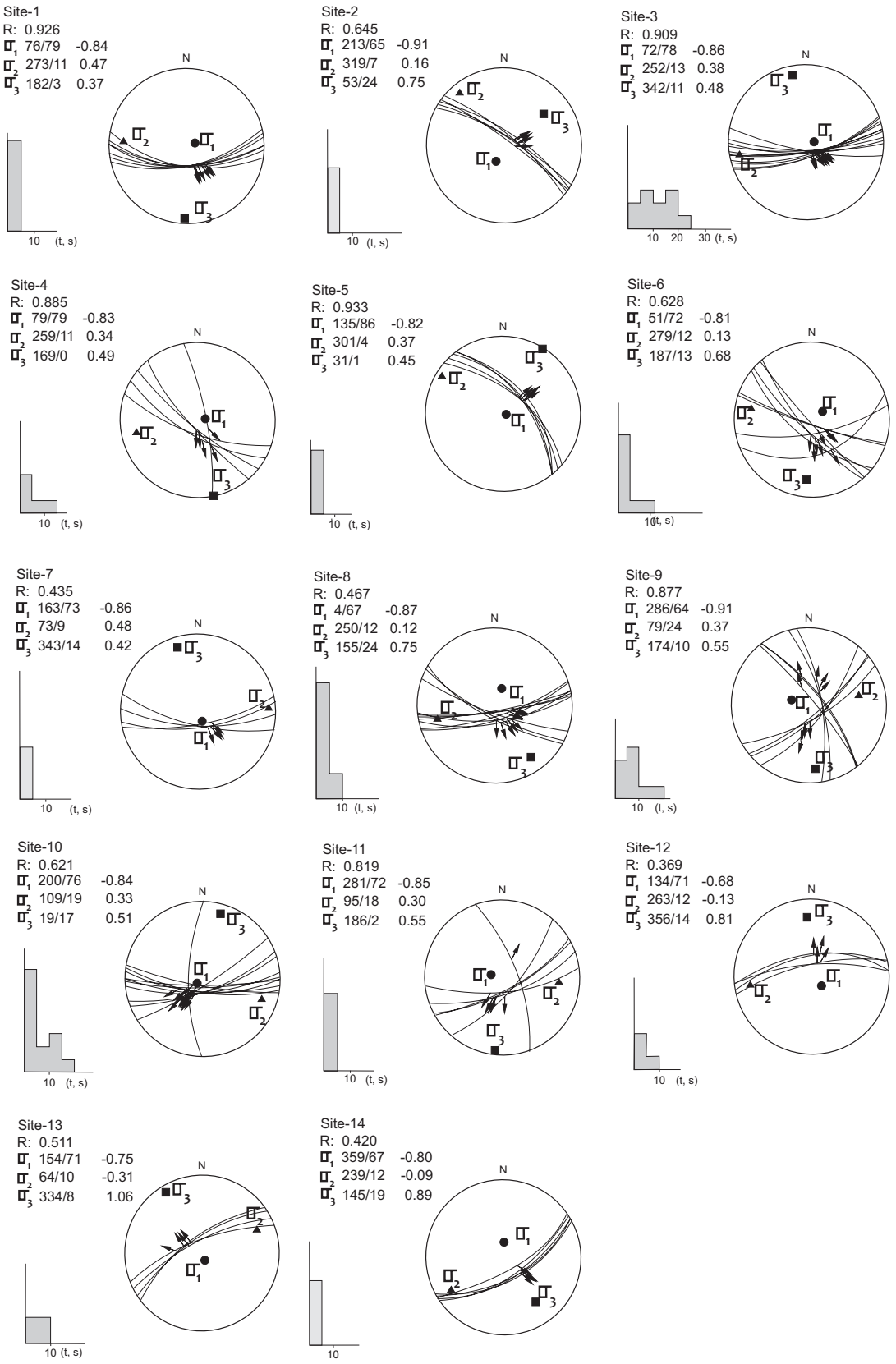

Fig. 12. The results of slip data stress tensor inversions reflect a normal fault stress regime with a σ_3 axis direction of approximately N–S black squares (σ_3), triangles (σ_2) and ball (σ_1) represent the stress axes obtained from the inversion. The histogram displays the distribution of deviation angles (angle between slip observed, s, and slip predicted, t). Labels outside the stereonets on the left refer to the position of the stereonets in Fig. 13 and which are mentioned in Table 2.

great earthquake, with a magnitude of Ms: 7.2, struck the islands of Amorgos and Santorini on July 9, 1956, 13 minutes apart (Makropoulos et al. 1989; Brüstle et al. 2014). The first earthquake, which occurred at a shallow depth and had a focal mechanism consistent with NW–SE extension, was mentioned in the previous paragraph. The body and surface wave amplitude ratios of the second event point to a source with intermediate depth of at least 100 km, which is compatible with Wadatti–Benioff Zone depths determined in the subducting Hellenic slab (Knapmeyer 1999; Papazachos et al. 2000; Meier et al. 2007; Brüstle 2012). The consistent fault plane solutions for this deep earthquake indicate a thrusting mechanism with a NE–SW trending P-axis and a steeply dipping T-axis (Brüstle et al. 2014), thereby supporting our findings from earthquakes deeper than 60 kilometers. Based on the fault-plane solutions method for intermediate-depth earthquakes (h>60 km) in the southern Aegean area, many researchers indicated thrust slab-events along the subducting Wadatti–Benioff Zone (Papazachos 1996; Papazachos et al. 2000; Brüstle et al. 2014; Kkalass et al. 2021). Indeed, compressional tectonics occur in the narrow intermediate depth (<60 km) of the Wadatti–Benioff Zone of the subducting African plate, while a roll-back event along the Hellenic Subduction Zone causes extensional tectonics in the upper plate (Aegean–Western Anatolia region).

Table 3: Location of kinematic sites with latitude, longitude, age, and lithology.

Sites	Latitude (N)	Longitude (E)	Age	Lithology
1	36°41'06"	27°23'13"	Pre-Neogene	ophiolitic–carbonate rock
2	36°46'11"	27°37'14"	Quaternary	continental clastics
3	36°46'41"	27°41'22"	Pliocene	continental clastics
4	36°46'33"	27°41'40"	Pliocene	continental clastics
5	36°43'50"	27°40'11"	Quaternary	continental clastics
6	36°46'46"	27°50'08"	Pre-Neogene	ophiolitic–carbonate rock
7	36°45'57"	27°43'35"	Pre-Neogene	ophiolitic–carbonate rock
8	36°45'21"	27°54'08"	Pre-Neogene	ophiolitic–carbonate rock
9	36°46'53"	28°00'12"	Pre-Neogene	ophiolitic–carbonate rock
10	36°47'24"	28°02'56"	Pre-Neogene	ophiolitic–carbonate rock
11	36°50'54"	28°12'54"	Pre-Neogene	ophiolitic–carbonate rock
12	36°43'29"	28°07'42"	Pre-Neogene	ophiolitic–carbonate rock
13	36°40'28"	28°04'01"	Pre-Neogene	ophiolitic–carbonate rock
14	36°38'30"	28°06'13"	Pre-Neogene	ophiolitic–carbonate rock

Conclusions

The kinematic analysis in and surrounding the Datça–Bozburun Peninsulas reflect the extensional regimes acting in the Southeastern Aegean which began during the Mio–Pliocene up to Present-day. The kinematic analysis of the faults measured in formations, aged from pre-Miocene up to Quaternary units, revealed the existence of extension regimes in N–S, NE–SW and NW–SE directions. On the other hand, the inversion of the focal mechanisms of the earthquakes occurring in the study area and its surroundings gives N–S and NW–SE extensions. The NW–SE trending Datça Peninsula was formed under the influence of the NE–SW extensional tectonic regime. The combined forces formed by the roll-back of the African Plate during the subduction process along the Hellenic Trench and the extrusion of Anatolia towards the south-southwest

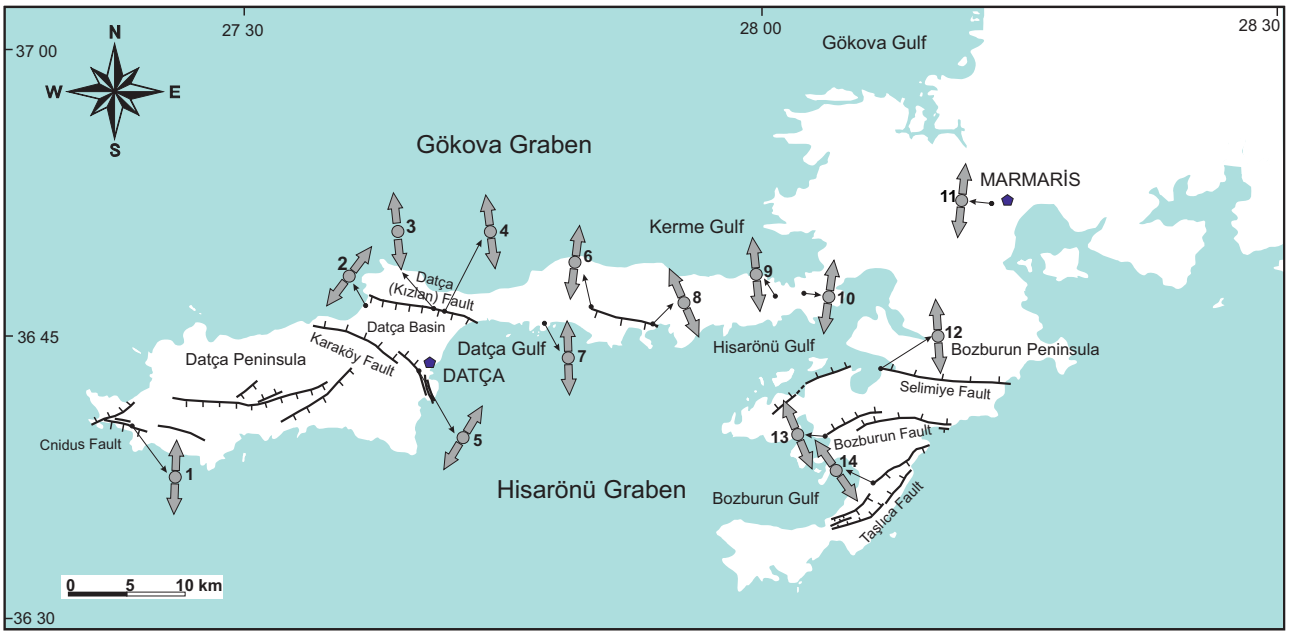

Fig. 13. The numbers show the location of the kinematic sites (Table 3) where the fault slips are measured and extension directions obtained from inversions (Fig. 12).

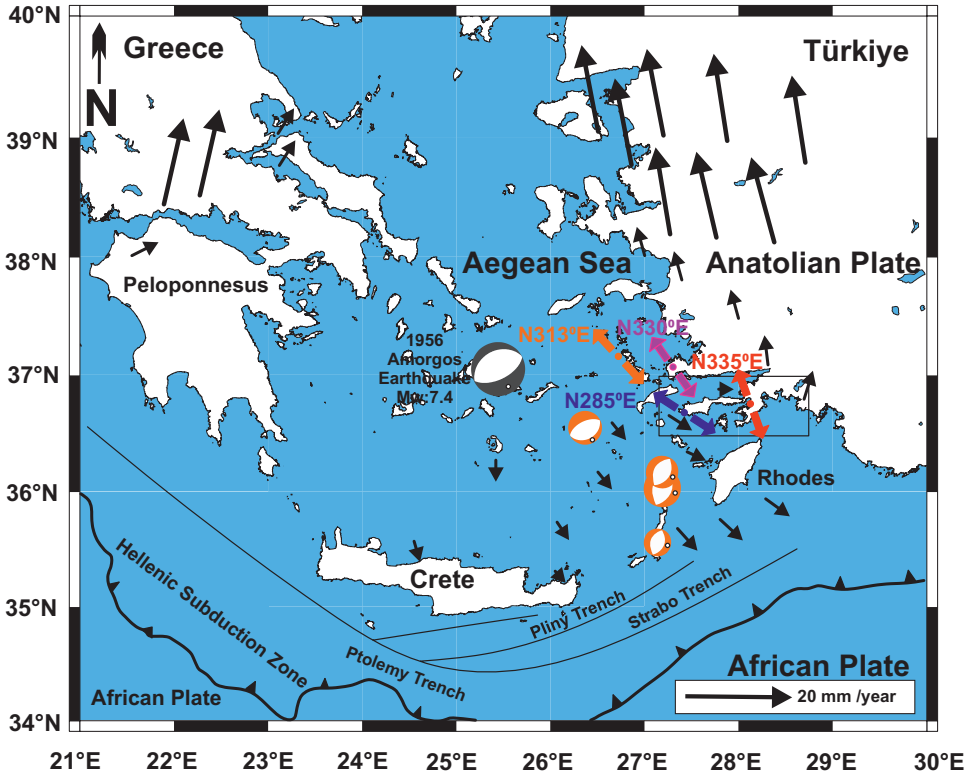

Fig. 14. Deformation pattern observed in the Southern Aegean region. Black arrows show GPS velocity vectors obtained with Aegean fixed (Reilinger et al. 2010). The orange-colored focal mechanisms were obtained from earthquakes larger than Mw≥5.0 from Bocchini et al. (2018). The black and white focal mechanism is the focal mechanism of the 1956 Amorgos earthquake (Mw=7.4) with the slip vector calculated on the SE dipping nodal plane. The NW–SE trending σ_3 axis calculated both from the inversion of the measured fault planes and of the shallow earthquakes in the Datça–Bozburun Peninsulas (see SFM 2, Table 2) are shown in red and blue respectively. The NW–SE trending σ_3 axis stress tensor shown in pink is from Över et al. (2021), and the orange one was obtained by Shah (2015) as a result of the inversion of the focal mechanisms of the shallow earthquakes that occurred in the northwest of Gökova Bay.

are responsible for the NE–SW and N–S extension regimes. The NW–SE extensional regime is due to the roll-back process of the African plate that occurred along the eastern branch of Hellenic Subduction Zone.

Acknowledgements: This study was supported by ÇOMÜ-BAP (FHD-2021-3736) as a research project. The authors would like to thank Catherine Yiğit for professional editing assistance with English exposition that improved the latest version of the text. We also thank the editor and anonymous reviewers for their valuable comments and suggestions, which improved the overall quality of the manuscript.

References

Akyol N., Zhu L., Mitchell B.J., Sözbilir H. & Kekovali K. 2006: Crustal structure and local seismicity in western Anatolia. *Geophysical Journal International* 166, 1259–1269. https://doi.org/10.1111/j.1365-246X.2006.03053.x

Alçicek C.M., Ten Veen H.J. & Özkul M. 2006: Neotectonic development of the Çameli basin, southwestern Anatolia, Turkey. *Geological Society, London, Special Publications* 260, 591–611. https://doi.org/10.1144/gsl.sp.2006.260.01.25

Ambraseys N.N. 1994: Material for the investigation of seismicity of central Greece. Materials CEC project. In: Albini P. & Moroni A. (eds.): *Review of Historical Seismicity in Europe* 2, 1–10.

Ambraseys N.N. & Finkel C.F. 1995: The seismicity of Turkey and adjacent areas. A historical review 1500–1800. *Eren Yayınevi*, İstanbul.

Ambraseys N.N. & White D. 1997: The Seismicity of the Eastern Mediterranean Region 550–1 BC: A Re-Appraisal. *Journal of Earthquake Engineering* 1, 603–632. https://doi.org/10.1080/13632469708962380

Angelier J. 1984: Tectonic analysis of fault slips data sets. *Journal of Geophysical Research* 80, 5835–5848. https://doi.org/10.1029/JB089iB07p05835

Angelier J. & Mechler E. 1977: Sur methode graphique de recherche des contraintes principales également utilisable en tectonique et en sismologie: la methode diédre droit. *Bulletin de la Société Geologique de France* 19, 1309–1318. https://doi.org/10.2113/gssgfbull.S7-XIX.6.1309

Angelier J., Dumont J.F., Karamenderesi H., Poisson A., Simsek S. & Uysal S. 1981: Analyses of fault mechanisms and expansion of south-western Anatolia since the Late Miocene. *Tectonophysics* 75, T1–T9. https://doi.org/10.1016/0040-1951(81)90271-7

Baes M., Govers R. & Wortel R. 2011: Switching between alternative responses of the lithosphere to continental collision. *Geophysical Journal International* 187, 1151–1174. https://doi.org/10.1111/j.1365-246X.2011.05236.x

Barka A. 1992: The Anatolian fault zone . *Annales Tectonicae* 6, 164–195.

Barka A.A. & Reilinger R. 1997: Active tectonics of the Mediterranean region: deduced from GPS, neotectonic and seismicity data. *Annali di Geophysica* XI, 587–610.

Bellier O. & Zoback M. 1995: Recent state of stress change in the Walker Lane zone western Basin and Range Province-USA. *Tectonics* 14, 564–593. https://doi.org/10.1029/94TC00596

Bellier O., Over S., Poisson A. & Andrieux J. 1997: Recent temporal change in the stress state and modern stress field along North Anatolian Fault Zone (Turkey). *Geophysical Journal International* 131, 61–86. https://doi.org/10.1111/j.1365-246X.1997.tb00595.x

Biryol C.B., Beck L.S., Zandt G. &, Özacar A.A. 2011: Segmented African lithosphere beneath the Anatolian region inferred from teleseismic P-wave tomography. *Geophysical Journal International* 184, 1037–1057. https://doi.org/10.1111/j.1365-246X.2010.04910.x

Bocchini G.M., Brüstle A., Becker D., Meier T., van Keken P.E., Ruscic M., Papadopoulos G.A., Rische M. & Friederich W. 2018: Tearing, segmentation, and backstepping of subduction in the Aegean: New insights from seismicity. *Tectonophysics* 734–735, 96–118. https://doi.org/10.1016/j.tecto.2018.04.002

Bohnhoff M., Rische M., Meier T., Becker D., Stavrakakis G. & Harjes H.P. 2006: Microseismic activity in the Hellenic Volcanic Arc, Greece, with emphasis on the seismotectonic setting of the Santorini-Amorgos zone. *Tectonophysics* 423, 17–33. https://doi.org/10.1016/j.tecto.2006.03.024

Bott M.H.P. 1959: The mechanism of oblique slip faulting. *Geological Magazine* 96, 109–117. https://doi.org/10.1017/S0016756800059987

Bouchon M. 1981: A simple method to calculate Green's functions for elastic layered media. *Bulletin of the Seismological Society of America* 71, 959–971. https://doi.org/10.1785/BSSA0710040959

Bousquet J.C. 1973: La tectonique récente de l'Apennin Calabro–Lucanien dans son cadre géologique et géophysique. *Geologica Romana* 12, 1–103.

Brüstle A. 2012: Seismicity of the eastern Hellenic Subduction Zone. *Ph. D. thesis, Fakultät für Geowissenschaften, Ruhr-Universität Bochum*.

Brüstle A., Friederich W., Meier T. & Gross C. 2014: Focal mechanism and depth of the 1956 Amorgos twin earthquakes from waveform matching of analogue seismograms. *Solid Earth* 5, 1027–1044. https://doi.org/10.5194/se-5-1027-2014

Carey E. 1979: Recherche des directions principales de contraintes associées au jeu d'une population de failles. *Revue Geological Dynamic and Géography Physic* 21, 57–66.

Carey E. & Brunier B. 1974: Analyse théorique et numérique d'une modéle méchanique élémentaire appliqué a l'étude d'une population de failles. *Comptes Rendus de l'Académie des Sciences Series D* 279, 891–894.

Carey-Gailhardis E. & Mercier J.L. 1987: A numerical method for determining the state of stress using source mechanisms of earthquake populations. *Earth and Planetary Science Letters* 82, 165–179. https://doi.org/10.1016/0012-821X(87)90117-8

Comninakis P. & Papazachos B. 1986: A catalogue of earthquakes in Greece and the surrounding area for the period 1901–1985. *University of Thessaloniki, Thessaloniki, Geophysical Laboratory Publications* 1, 1–167

Çelikkol Z. 1990: İstanköy'deki Türk Eserleri ve Tarihçe. Atatürk Kültür, Dil ve Tarih Yüksek Kurumu. *Türk Tarih Kurumu, Yayınları* 6 (39), Ankara (in Turkish).

Çelikkol Z. 1992: Rodos'taki Türk Eserleri ve Tarihçe. *Türk Tarih Kurumu, Yayınları*, Ankara, 1–23 (in Turkish).

Dewey J.F. & Şengör A.M.C. 1979: Aegean and Surrounding Regions–Complex Multi-Plate and Continuum Tectonics in a Convergent Zone. *Geological Society of America Bulletin* 90, 89–92. https://doi.org/10.1130/0016-7606(1979)90%3C84:AASRCM%3E2.0.CO;2

Dilek Y. & Altunkaynak Ş. 2009: Geochemical and temporal evolution of Cenozoic magmatism in western Turkey: mantle response to collision, slab break-off, and lithospheric tearing in an orogenic belt. *Geological Society, London, Special Publications* 311, 213–233. https://doi.org/10.1144/SP311.8

Dirik K. 2007: Neotectonic characteristics and seismicity of the Reşadiye Peninsula and surrounding area, Southwest Anatolia. *Geological Bulletin of Turkey* 50, 130–149.

Emre Ö., Duman T.Y. & Özalp S. 2013: 1:250.000 Ölçekli Türkiye Diri Fay Haritaları Serisi. *Maden Tetkik ve Arama Genel Müdürlüğü*, Ankara, Türkiye.

Ergin K., Güçlü U. & Uz Z. 1967: A Catalog of Earthquakes for Turkey and Surrounding Area (11 A.D. to 1964 A.D.). *Technical Report, İstanbul Technical University, Faculty of Mines, Institute of Physics of the Earth*, no. 24.

Ersoy Ş. 1990: Datça Yarımadasının stratigrafisi ve tektoniği. *Türkiye Jeoloji Bülteni* 34, 1–14.

Eyidoğan H. & Barka A. 1996: The 1 October 1995 Dinar earthquake, SW Turkey. *Terra Nova* 8, 479–485. https://doi.org/10.1111/j.1365-3121.1996.tb00773.x

Faccenna C., Piromallo C., Crespo Blanc A., Jolivet L. & Rossetti F. 2004: Lateral slab deformation and the origin of the arcs of the western Mediterranean. *Tectonics* 23, TC1012. https://doi.org/10.1029/2002TC001488

Govers R. & Fichtner A. 2016: Signature of slab fragmentation beneath Anatolia from fullwaveform tomography. *Earth and Planetary Science Letters* 450, 10–19. https://doi.org/10.1016/j.epsl.2016.06.014

Govers R. & Wortel M.J.R. 2005: Lithosphere tearing at STEP faults: response to edges of subduction zones. *Earth and Planetary Science Letters* 236, 505–523. https://doi.org/10.1016/j.epsl.2005.03.022

Guidoboni E., Comastri A. & Triana G. 1994: Catalogue of Ancient Earthquakes in the Mediterranean Area up to the 10th Century. *Istituto Nazionale di Geofisica*, 1–504.

Gürsoy H., Kürçer A. & Domaç Yalçın H. 2022: Ege Denizi'nde bir denizaltı volkanı mı doğuyor? *Mavi Gezegen* 30, 31–39 (in Turkish).

Jackson J. & Mc Kenzie D.P. 1984: Active tectonics of the Alpine–Himalayan belt between western Turkey and Pakistan. *Geophysical Journal Royal Astronomy Society* 77, 185–264. https://doi.org/10.1111/j.1365-246X.1984.tb01931.x

Jackson J. & Mc Kenzie D.P. 1988: The relationship between plate motion and seismic moment tensors, and the rates of active deformation in the Mediterranean and Middle-East. *Geophysical Journal Royal Astronomy Society* 93, 45–73. https://doi.org/10.1111/j.1365-246X.1988.tb01387.x

Jolivet L. & Brun J.P. 2010: Cenozoic geodynamic evolution of the Aegean. *International Journal of Earth Sciences* 99, 109–138. https://doi.org/10.1007/s00531-008-0366-4

Karasözen E., Nissen E., Büyükakpınar P., Cambaz M.D., Kahraman M., Ertan E.S., Abgarmi B., Bergman B., Ghods A., Özacar A.A. 2018: The 2017 July 20 Mw 6.6 Bodrum-Kos earthquake illuminates active faulting in the Gulf of Gökova, SW Turkey. *Geophysical Journal International* 214, 185–199. https://doi.org/10.1093/gji/ggy114

Kassaras I., Kapetanidis V., Ganas A., Tzanis A., Kosma C., Karakonstantis A., Valkaniotis S., Chailas S., Kouskouna V. & Papadimitriou P. 2020: The new seismotectonic atlas of Greece (v1.0) and its implementation. *Geosciences* 10, 447. https://doi.org/10.3390/geosciences10110447

Kikuchi M. & Kanamori H. 1991: Inversion of complex body waves – III. *Bulletin of the Seismological Society of America* 81, 2335–2350. https://doi.org/10.1785/BSSA0810062335

Kkallas C., Papadimitriou P., Karakostas V. & Papazachos C. 2021: Strong earthquakes recurrence times of the Southern Thessaly,

Greece, fault system: Insights from a physics-based simulator application. *Frontiers in Earth Science* 9, 596854. https://doi.org/10.3389/feart.2021.596854

Knapmeyer M. 1999: Geometry of the Aegean Benioff zones. Annals of Geophysics 42. https://doi.org/10.4401/ag-3697

Kürçer A. & Gürsoy H. 2023: Yatağan fayının aktif tektonik özellikleri ve Holosen paleosismolojik tarihçesi, Güneybatı Anadolu, Türkiye. *MTA Yerbilimleri ve Madencilik Dergisi* 2, 87–112 (in Turkish). https://doi.org/10.52998/mta.1264629

Le Pichon X. 1982: Land-locked oceanic basins and continental collision: eastern Mediterranean as a case example. In: Hsü K. (Ed.): Mountain Building Processes. *Academic Press*, New York, 201–211.

Le Pichon X. & Angelier J. 1979: The Hellenic arc and trench system: a key to the evolution of eastern Mediterranean area. *Tectonophysics* 60, 1–42. https://doi.org/10.1016/0040-1951(79)90131-8

Le Pichon X., Chamot-Rooke N., Lallemant S., Noomen R. & Veis G. 1995: Geodetic determination of the kinematics of central Greece with respect to Europe: Implications for eastern Mediterranean tectonics. *Journal of Geophysical Research* 100, 12675–12690. https://doi.org/10.1029/95JB00317

Leite O. & Mascle J. 1982: Geological structures on the South Cretan continental margin and Hellenic Trench (eastern Mediterranean). *Marine Geology* 48, 199–223. https://doi.org/10.1016/0025-3227(82)90040-8

Luttrell A. 1999: Earthquakes in the Dodecanese: 1303–1512. In: Zachariadon E. (Ed.): Natural Disasters in the Ottoman Empire (Rethymnon, 1999), repr. In Luttrell, Studies, no. X, 145–151.

Makropoulos K.C., Drakopoulos J. & Latoussakis J.B. 1989: A revised and extended earthquake catalogue in Greece since 1900. *Geophysical Journal International* 98, 391–394. https://doi.org/10.1111/j.1365-246X.1989.tb03360.x

Malinverno A. & Ryan W.B.F. 1986: Extension in the Tyrrhenian Sea and shortening in the Apennines as result of arc migration driven by sinking of the lithosphere. *Tectonics* 5, 227–245. https://doi.org/10.1029/TC005i002p00227

Mascle J., Le Quellec P., Leité O. & Jongsma D. 1982: Structural Sketch of the Hellenic Continental-Margin Between the Western Peloponnesus and Eastern Crete. *Geology* 10, 113–116. https://doi.org/10.1130/0091-7613(1982)10%3C113:SSOTHC%3E2.0.CO;2

Mascle J., Cousin M., Fleury J.J., Le Cleac'h A.G. & Saint-Marc P. 1986: Mesozoic Limestones Within the Hellenic Trench – Paleogeographic and Geodynamic Implications. *Marine Geology* 73, 323–341. https://doi.org/10.1016/0025-3227(86)90021-6

McClusky S. et al. (25 authors) 2000: Global Positioning System constraints on plate kinematics and dynamics in the eastern Mediterranean and Caucasus. *Journal of Geophysical Research, Solid Earth* 105, 5695–5719. https://doi.org/10.1029/1999JB900351

McClusky S., Reilinger R., Mahmoud S. Ben Sari D. & Tealeb A. 2003: GPS constraints on Africa (Nubia) and Arabia plate motions. *Geophysical Journal International* 155, 126–138. https://doi.org/10.1046/j.1365-246X.2003.02023.x

McKenzie D. 1972: Active tectonics of the Mediterranean Region. *Geophysical Journal of Royal Astronomical Society* 30, 109–185. https://doi.org/10.1111/j.1365-246X.1972.tb02351.x

Meier T., Becker D., Endrun B., Rische M., Bohnhoff M., Stöckert B. & Harjes H.-P. 2007: A model for the Hellenic subduction zone in the area of Crete based on seismological investigations. *Geological Society, London, Special Publications* 291, 183–199. https://doi.org/10.1144/SP291.9

Mercier J.L. 1981: Extensional–compressional tectonics associated with the Aegean Arc: comparison with the Andean Cordillera of south Peru–North Belivia. *Philosophical Transactions of the Royal Society London A* 300, 337–355. https://doi.org/10.1098/rsta.1981.0068

Mercier J.L., Delibassis N., Gauthier A., Jarrige J.J., Lemeille F., Philip H., Sebrier M. & Sorel D. 1979: La néotectonique de l'Arc Egéen. *Revue de Géologie Dynamique et de Géographie Physique* 21, 67–92.

Mercier J.L., Sorel D. & Vergely P. 1989: Extensional tectonic regimes in the Aegean basins during the Cenozoic. *Basin Research* 2, 49–71. https://doi.org/10.1111/j.1365-2117.1989.tb00026.x

Mercier J.L., Carey-Gailhardis E. & Sebrier M. 1991: Paleostress determinations from fault kinematics: application to the Neotectonics of the Himalayas–Tibet and the Central Andes. *Philosophical Transactions of the Royal Society London A* 337, 41–52. https://doi.org/10.1098/rsta.1991.0105

Ocakoğlu N., Nomikou P., İşcan Y., Loreto M.F. & Lampridou D. 2018: Evidence of extensional and strike-slip deformation in the offshore Gökova-Kos area affected by the July 2017 Mw:6.6 Bodrum-Kos earthquake, eastern Aegean Sea. *Geo-Marine Letters* 38, 211–225. https://doi.org/10.1007/s00367-017-0532-4

Okal E., Synolakis C., Uslu B., Kalligeris N. & Voukouvalas E. 2009: The 1956 earthquake and tsunami in Amorgos, Greece. *Geophysical Journal International* 178, 1533–1554. https://doi.org/10.1111/j.1365-246X.2009.04237.x

Över S., Ünlügenç U.C. & Bellier O. 2002: Quaternary stress regime changes in the Hatay region (SE Turkey). *Geophysical Journal International* 148, 1–14. https://doi.org/10.1046/j.1365-246X.2002.01621.x

Över S., Özden S., & Unlügenc U. 2004: Late Cenozoic stress distribution along the Misis Range in the Anatolian, Arabian, and African plate intersection region, SE Turkey. *Tectonics* 23, TC3008. https://doi.org/10.1029/2002TC001455

Över S., Pınar A., Özden S., Yılmaz, H., Ünlügenç U.C. & Kamacı Z. 2010: Late Cenozoic Stress Field in the Çameli Basin, SW Turkey. *Tectonophysics* 492, 60–72. https://doi.org/10.1016/j.tecto.2010.04.037

Över S., Özden S., Yılmaz H., Pınar A., Ünlügenç U.C. & Kamacı Z. 2013a: Plio–Quaternary stress regime in Esen Çay Basin, SW Turkey. *Geological Society, London, Special Publications* 372, 547–560. https://doi.org/10.1144/SP372.24

Över S., Yılmaz H., Pınar A., Özden S., Ünlügenç U.C. & Kamacı Z. 2013b: Plio–Quaternary stress state in the Burdur Basin, SW Turkey. *Tectonophysics* 588, 56–68. https://doi.org/10.1016/j.tecto.2013.03.020

Över S., Özden S., Pınar A., Yılmaz H., Kamacı Z. & Ünlügenç U.C. 2016: Late Cenozoic Stress State distributions at the intersection of the Hellenic and Cyprus Arcs, SW Turkey. *Journal of Asian Earth Sciences* 132, 94–102. https://doi.org/10.1016/j.jseaes.2016.10.003

Över S., Özden S., Ertan E., Turhan F., Coşkun Z. & Pınar A. 2021: The 20 July 2017 Bodrum-Kos Earthquake (Mw 6.6) in southwestern Anatolia, Turkey. *Earth Sciences Research Journal* 25, 309–321. https://doi.org/10.15446/esrj.v25n3.87080

Özbakır A.D., Şengör A.M.C., Wortel M.J.R. & Govers R. 2013: The Pliny–Strabo trench region: A large shear zone resulting from slab tearing. *Earth and Planetary Science Letters* 375, 188–195. https://doi.org/10.1016/j.epsl.2013.05.025

Özden S., Över S., Altuncu Poyraz S., Güneş Y. & Pınar A. 2018: Tectonic implications of the 2017 Ayvacık (Çanakkale) earthquakes, Biga Peninsula, NW Turkey. *Journal of Asian Earth Sciences* 154, 125–141. https://doi.org/10.1016/j.jseaes.2017.12.021

Özsayın E., Üner S. & Kahraman B. 2021: Late Quaternary subsidence records from the Datça graben and Cnidus ancient city (SW Turkey): Sea-Level Changes versus Tectonics. *Geologica Acta* 19, 1–14. https://doi.org/10.1344/GeologicaActa2021.19.6

Papazachos B.C. 1973: Distribution of Seismic Foci in the Mediterranean and Surrounding Area and its Tectonic Implication. *Geophysical Journal Royal Astronomy Society* 33, 421–430. https://doi.org/10.1111/j.1365-246X.1973.tb02377.x

Papazachos B.C. 1996: Large seismic faults in the Hellenic arc. *Annali di Geofisica* 39. https://doi.org/10.4401/ag-4023

Papazachos B.C., Karakostas V.G., Papazachos C.B. & Scoridilis E.M. 2000: The geometry of the Wadati-Benioff zone and lithospheric kinematics in the Hellenic arc. *Tectonophysics* 319, 275–300. https://doi.org/10.1016/S0040-1951(99)00299-1

Papazachos B.C., Comninakis P.E., Scordilis E.M., Karakaisis G.F. & Papazachos C.B. 2010: A Catalogue of Earthquakes in the Mediterranean and Surrounding Area for the Period 1901–2010. *Publication of the Geophysical Laboratory, University of Thessaloniki*.

Papazachos C. & Nolet G. 1997: P and S deep velocity structure of the Hellenic area obtained by robust nonlinear inversion of travel times. *Journal of Geophysical Research* 102, 8349–8367. https://doi.org/10.1029/96JB03730

Philip H. 1987: Plio-Quaternary Evolution of the Stress-Field in Mediterranean Zones of Subduction and Collision. *Annales Geophysicae Series B – Terrestrial and Planetary Physics* 5, 301–319.

Reilinger R. & Barka A.A. 1997: GPS constraints on slip rates in the Arabia–Africa–Eurasia plate collision zone: Implications for the earthquake recurrence times. *NATO ASI Series* 28, 91–108.

Reilinger R.E., McClusky S.C., Oral M.B., King R.W. & Toksöz M.N. 1997: Global Positioning System measurements of present-day crustal movements in the Arabia–Africa–Eurasia plate collision zone. *Journal of Geophysical Research* 102, 9983–9999. https://doi.org/10.1029/96JB03736

Reilinger R., McClusky S. et al. (12 authors) 2006: GPS constraints on continental deformation in the Africa–Arabia–Eurasia continental collision zone and implications for the dynamics of plate interactions. *Journal of Geophysical Research* 111, B05411. https://doi.org/10.1029/2005JB004051

Reilinger R., McClusky S., Paradissis D., Ergintav S. & Vernant P. 2010: Geodetic constraints on the tectonic evolution of the Aegean region and strain accumulation along the Hellenic subduction zone. *Tectonophysics* 488, 22–30. https://doi.org/10.1016/j.tecto.2009.05.027

Robertson A.H.F. 1990: Tectonic evolution of Cyprus. In: Moores E.M. et al. (eds.): Ophiolites and Oceanic Lithosphere. *Proc. Int. Symp.* Nicosia, 235–250.

Royden L.H. 1993: The tectonic expression of slab pull at continental convergent boundaries. *Tectonics* 12, 303–325. https://doi.org/10.1029/92TC02248

Seyitoğglu G., Karabıyıkoglu T., Kaypak B., Tanülkü E. & Koca B. 2024: Influence Pliny-Strabo Fault Zone in Bozburun Peninsula (Southwest Türkiye): Evidence from Structural Data and Focal Mechanism Solutions. *Geological Bulleltin of Turkey* 67. https://doi.org/10.25288/tjb.1341249

Shah A.A. 2015: Kashmir basin fault and its tectonic significance in NW Himalaya, Jammu and Kashmir, India. *International Journal of Earth Sciences* 104, 1901–1906. https://doi.org/10.1007/s00531-015-1183-1

Shaw B. & Jackson J. 2010: Earthquake mechanisms and active tectonics of the Hellenic subduction zone. *Geophysical Journal International* 181, 966–984. https://doi.org/10.1111/j.1365-246X.2010.04551.x

Sodoudi F., Brüstle A., Meier T., Kind R. & Friederich W. 2015: Receiver function images of the Hellenic subduction zone and comparison to microseismicity. *Solid Earth* 6, 135–151. https://doi.org/10.5194/se-6-135-2015

Sokos E.N. & Zahradnik J. 2008: ISOLA a Fortran code and a Matlab GUI to perform multiple-point source inversion of seismic data, *Computers & Geosciences* 34, 967–977. https://doi.org/10.1016/j.cageo.2007.07.005

Sorel D., Mercier J.L., Keraudren B. & Cushing M. 1988: Le role de la traction de la Lithosphere Subducte dans l'evolution Geodynamique Plio-Pleistocene de l'Arc Egeen: Mouvement Verticaux Alternes et Variations du Regime Tectonique. *Comptes Rendus Geosciences* 307, 1981–1986.

Soukis K. & Gouliotis L. 2018: Faulting pattern and paleostress analysis on Symi Island (Dodecanese Islands, Greece). *Journal of Structural Geology* 114, 1–15.

Sözbilir H., Sarı B., Uzel B., Sümer Ö. & Akkiraz S. 2011: Tectonic implications of transtensional supradetachment basin development in an extension-parallel transfer zone: The Kocaçay Basin, western Anatolia, Turkey. *Basin Research* 23, 423–448. https://doi.org/10.1111/j.1365-2117.2010.00496.x

Şenel M. 1997: Geological Map of Turkey, Burdur Sheet (No. 19). *General Directorate of Mineral Research and Exploration (MTA)*, Ankara.

Taymaz T., Jackson J. & McKenzie D. 1991: Active tectonics of the north and central Aegean Sea. *Journal of Geophysical Research* 106, 433–490. https://doi.org/10.1111/j.1365-246X.1991.tb03906.x

Taymaz T., Yolsal-Çevikbilen S., Irmak T.S., Vera F., Liu C.L .,Eken T., Zhang Z.G. Erman C. & Keles D. 2022: Kinematics of the 30 October 2020 *Mw 7.0* Neon Karlovasion (Samos) earthquake in the Eastern Aegean Sea: Implications on source characteristics and dynamic rupture simulations. *Tectonophysics* 826, 229223. https://doi.org/10.1016/j.tecto.2022.229223

ten Veen J. & Kleinspehn K.L. 2002: Geodynamics along an increasingly curved convergent platemargin: Late Miocene–Pleistocene Rhodes, Greece. *Tectonics* 21, 1017. https://doi.org/10.1029/2001TC001287

ten Veen J.H., Woodside J.M., Zitter T.A.C., Dumont J.-F., Mascle J. & Volkonskaia A. 2004: Neotectonic evolution of the Anaximander Mountains at the junction of the Hellenic and Cyprus arcs. *Tectonophysics* 391, 35–65. https://doi.org/10.1016/j.tecto.2004.07.007

ten Veen J.H., Boulton S.J. & Alcicek M.C. 2009: From palaeotectonics to neotectonics in the Neotethys realm: the importance of kinematic decoupling and inherited structural grain in SW Anatolia (Turkey). *Tectonophysics* 473, 261–281. https://doi.org/10.1016/j.tecto.2008.09.030

Tiryakioğlu İ., Aktuğ B., Yiğit C.Ö., Yavaşoğlu H.H., Sözbilir H., Özkaymak Ç., Poyraz F., Tanelia E., Bulut F., Doğru A. & Özener H. 2018: Slip distribution and source parameters of the 20 July 2017 Bodrum-Kos earthquake (Mw:6.6) from GPS observations. *Geodinamica Acta* 30, 1–14. https://doi.org/10.1080/09853111.2017.1408264

Tur H., Demirtaş R. & Kaya Ö. 2015: Pliocene–Quaternary tectonic evolution of the Gulf of Gökova, southwest Turkey. *Tectonophysics* 638, 158–176. https://doi.org/10.1016/j.tecto.2014.11.008

Uluğ A., Duman M., Ersoy Ş., Özel E. & Avcı M. 2005: Late Quaternary sea-level change, sedimentation and neotectonics of the Gulf of Gökova: Southeastern Aegean Sea. *Marine Geology* 221, 381–395. https://doi.org/10.1016/j.margeo.2005.03.002

Van Hinsbergen J.J., Dekkers M.J., Bozkurt E. & Koopman M. 2010: Exhumation with a twist: Paleomagnetic constraintson the evolution of the Menderes metamorphiccore complex, western Turkey. *Tectonics* 29. https://doi.org/10.1029/2009TC002596

Wortel M.J.R. & Spakman W. 2000: Subduction and Slab Detachment in the Mediterranean-Carpathian Region. *Science* 290, 5498, 1910–1917. https://doi.org/10.1126/science.290.5498.1910

Yolsal S. & Taymaz T. 2010: Sensitivity analysis on relations between earthquake source rupture parameters and far-field tsunami waves: case studies in the Eastern Mediterranean Region. *Turkish Journal of Earth Sciences* 19, 313–349. https://doi.org/10.3906/yer-0902-8

Yolsal S., Taymaz T. & Yalçıner A.C. 2007: Understanding tsunamis, potential source regions and tsunami prone mechanisms in the Eastern Mediterranean. *Geological Society, London, Special Publications* 29, 201–230. https://doi.org/10.1144/sp291.10